

# INTER: Mitigating Hallucination in Large Vision-Language Models by Interaction Guidance Sampling

Xin Dong<sup>\*,1,2</sup>, Shichao Dong<sup>\*,2</sup>, Jin Wang<sup>\*,3</sup>, Jing Huang<sup>†,1</sup>, Li Zhou<sup>2</sup>, Zenghui Sun<sup>2</sup>,  
Lihua Jing<sup>1</sup>, Jinsong Lan<sup>2</sup>, Xiaoyong Zhu<sup>2</sup>, Bo Zheng<sup>†,2</sup>

<sup>1</sup>University of Chinese Academy of Sciences

<sup>2</sup>Taobao & Tmall Group of Alibaba

<sup>3</sup>The University of Hong Kong  
dongxin@ie.ac.cn

## Abstract

Hallucinations in large vision-language models (LVLMs) pose significant challenges for real-world applications, as LVLMs may generate responses that appear plausible yet remain inconsistent with the associated visual content. This issue rarely occurs in human cognition. We argue that this discrepancy arises from humans' ability to effectively leverage multimodal interaction information in data samples. Specifically, humans typically first gather multimodal information, analyze the interactions across modalities for understanding, and then express their understanding through language. Motivated by this observation, we conduct extensive experiments on popular LVLMs and obtained insights that surprisingly reveal human-like, though less pronounced, cognitive behavior of LVLMs on multimodal samples. Building on these findings, we further propose **INTER: Interaction Guidance Sampling**, a novel training-free algorithm that mitigate hallucinations without requiring additional data. Specifically, **INTER** explicitly guides LVLMs to effectively reapply their understanding of multimodal interaction information when generating responses, thereby reducing potential hallucinations. On six benchmarks including VQA and image captioning tasks, **INTER** achieves an average improvement of up to 3.4% on five LVLMs compared to the state-of-the-art decoding strategy. The code will be released when the paper is accepted.

## 1. Introduction

Large Vision-Language Models (LVLMs) have demonstrated remarkable versatility across a wide range of tasks, from image captioning to complex reasoning [3, 10, 13,

\* Equal Contribution.

† Corresponding authors.

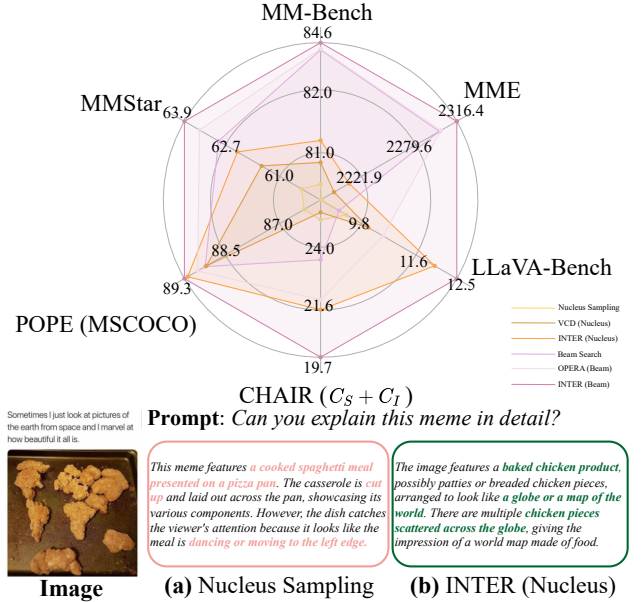


Figure 1. Comparisons with existing decoding strategies on the state-of-the-art LVLM InternVL2.5-MPO [10]. Our approach INTER achieved optimal results across six benchmarks. Besides, the detailed output of INTER in a case of complex inputs is presented. The hallucinated words are highlighted in red.

31, 38, 63]. These models blend visual and textual information, enhancing our ability to interpret and interact with the world. However, LVLMs experience hallucinations that hinder their applications, which means that responses are not aligned with the given input [8, 11, 16, 25, 30, 50, 55].

Previous methods made attempts to address this issue with additional training and fine-grained data [29, 36, 50, 65–67], but such approaches often demand substantial human effort and computational resources. In parallel, other methods were proposed to explore efficient training-free

methods to mitigate hallucinations in LVLMS [1, 11, 16, 17, 25, 40, 42, 72]. These methods aimed to enhance the model’s focus on the input *visual* or *textual* information by adjusting the logit distribution during the autoregressive generation process, thereby reinforcing the link between the output and *uni-modal* information.

Despite these efforts, the role of *multimodal interactions* information in shaping LVLMS’ hallucinated responses remains largely underexplored, even though it naturally plays a critical role in human cognition for accurate reasoning. Specifically, when presented with a textual prompt and an associated image, humans typically first gather multimodal information, analyze the interactions between modalities to form a conceptual understanding, and then provide textual responses based on this understanding.

Motivated by this intuition, we propose to first investigate whether LVLMS exhibit similar cognitive behavior when processing multimodal data, aiming to uncover the potential causes behind their hallucination issues. To this end, we designed several metrics based on the Harsanyi dividend [22] to explicitly quantify the influence of image-text multimodal interactions in LVLMS’ responses. The Harsanyi dividend was originally proposed in game theory, which measures the interactions among different players. Associated with the Shapley value [48], the Harsanyi dividend theoretically satisfies the *efficiency*, *linearity*, *dummy*, *symmetry* axioms, which further enhances its trustworthiness on the analyses of LVLMS [44, 45, 56].

In this way, we derive the following key insights through extensive analysis:

- **Insight 1: LVLMS implicitly capture multimodal interactions from input samples and leverage such interactions for decision-making to some extent.**
- **Insight 2: LVLMS exhibit a tendency to primarily apply their understanding of multimodal interactions to the generation of a few key tokens, rather than uniformly across all response tokens.**
- **Insight 3: The understanding of multimodal interactions in LVLMS positively influences the quality of generated responses, with stronger interactions leading to greater accuracy.**

To our surprise, the above findings suggest that LVLMS possess a human-like—albeit less pronounced—understanding of multimodal interactions, which inspired us to design *efficient* methods for reducing hallucinated responses of LVLMS.

To mitigate the hallucinations of LVLMS, we propose a simple yet effective method named **INTER: Interaction Guidance Sampling**, which aims to reapply their captured multimodal interaction understanding (*cf. Insight 1*) more accurately and effectively in LVLMS’ reasoning process. Specifically, we first design a variance-based filtering module termed as the Interactive Guided Locator in INTER to

automatically detect key tokens that significantly contribute to the accuracy of responses (*cf. Insight 2*). After that, we design the Interaction Probability Modifier in INTER which guides the sampling of these key tokens to rely more on multimodal interactions (*cf. Insight 3*). In this way, LVLMS can reduce potential hallucinations in their responses, improving their overall performance.

As shown in Fig. 1, our INTER achieved better performance on the state-of-the-art LVLMS InternVL2.5-MPO (8B) [10] across six widely-used benchmarks [7, 19, 33, 37, 39, 46]. In experiments, we also verified the effectiveness of INTER on other popular LVLMS [3, 9, 13, 38, 63]. Specifically, INTER boosted the performance of state-of-the-art decoding strategies by an average of 4.1% and 2.6% on CHAIR [46] and MME [19] benchmark, respectively.

Our contributions can be summarized as follows:

- From a novel game-theoretic view, we propose to investigate the roles of multimodal interactions in shaping LVLMS’ hallucinated responses. Through extensive analyses, we obtain several new insights accordingly.
- We propose Interaction Guidance Sampling (INTER), a novel plug-and-play sampling rectification method for eliminating hallucinations, that accurately and effectively guides LVLMS to explicitly reapply their understanding of multimodal interactions in responses.
- Extensive experiments demonstrate that INTER successfully improved the performance of various LVLMS upon six benchmarks without requiring additional training, outperforming state-of-the-art methods by a large margin.

## 2. Related Work

### 2.1. Large Vision-Language Models (LVLMS)

The rapid advancement of Large Vision-Language Models (LVLMS) has become a pivotal area in artificial intelligence research. These models aim to generate contextually grounded responses through multimodal understanding. Modern architectures typically adapt existing Large Language Models (LLMs) as text decoder for generation. Prominent examples include LLaVA-v1.5 [38] and InstructBLIP [13], both built on Vicuna 7B [12], as well as Qwen-VL [3] and mPLUG-Owl2 [63], which utilize Qwen 7B [2] and LLaMA 2 7B [54] respectively. Scalability efforts are exemplified by InternVL2 [10], which explores parameter configurations from 1B to 108B. Despite these advancements, a critical challenge persists: hallucination, where generated responses exhibit inconsistencies with input [8, 11, 16, 25, 30, 41, 50, 55]. This phenomenon underscores fundamental challenges in multimodal understanding that demand further investigation.

## 2.2. Mitigating Hallucinations in LVLMS

Given the substantial time costs associated with data preparation and model training, current approaches [1, 11, 16, 17, 25, 27, 40, 42, 72] primarily address hallucination during inference. Most of them employ contrastive decoding [32] to rectify the original logit distribution, thereby enhancing model attention to input uni-modal information. Specifically, VCD [16] enhances the probabilities of input-relevant tokens by contrasting logit distributions between hallucination-prone masked images and original images. OPERA [25] found that partial overtrust tendencies lead to hallucinations. An over-trust logit penalty was introduced in the decoding phase to increase the focus of LVLMS on image tokens, thereby alleviating the hallucinations. Unlike these methods that emphasize reinforcing the focus on uni-modal information, our work focuses on mitigating hallucination by enhancing the role of multimodal interactions in decision-making of LVLMS. Through comparison with existing state-of-the-art methods across multiple benchmarks, we have demonstrated the effectiveness of our method.

## 2.3. Interactions of DNNs

In recent years, an increasing number of studies have focused on quantifying the interactions among input units to analyze the representations of deep neural networks (DNNs) [20, 22, 48, 52]. Several studies [43, 57, 58] focused on interpret the adversarial transferability and adversarial attacks of DNNs with interactions metrics. Other research explained the generalization power of DNNs from the perspective of interactions [70, 71]. Furthermore, certain works [69, 70] extended interactions metrics to account for multi-order and multivariate interactions, which have also been applied to explain various phenomena in DNNs [6, 14, 15, 61, 68]. Different from above studies, our work focuses on analyzing the hallucination issues in Large Vision-Language Models (LVLMS) from the perspective of multimodal interactions, which still remained largely under-explored in the past literature.

## 3. Multimodal Interactions in LVLMS

In this section, we expect to investigate the roles of multimodal interactions in shaping LVLMS' responses, with the goal of identifying potential causes of their hallucination issues. Specifically, we propose to first verify the existence of interactions within LVLMS' responses, then locate the scope of such interactions in LVLMS' responses, and finally evaluate the impact of such interactions on the generated responses. To conduct the above analyses, we designed several metrics based on the Harsanyi dividend [22], for which we present a brief introduction for better understanding.

## 3.1. The Harsanyi Dividend

The Harsanyi dividend is a metric from game theory used to quantify the contribution of a coalition composed of multiple players to a game. Specifically, given a set of players  $\mathcal{N}$  participating in a game  $L$ , these players may obtain a certain reward  $L(\mathcal{N})$ , where  $L(\cdot)$  can be considered as a reward function mapping any subset of players  $A \subseteq \mathcal{N}$  to a numerical value. Under this context, each player usually does not participate in the game individually, but forms different coalitions with extra interaction effects, contributing to the final reward. Mathematically, such effects of interactions can be uniquely measured by the Harsanyi dividend, which is defined as follows,

$$I(A|\mathcal{N}) = \sum_{A' \subseteq A} (-1)^{|A'| - |A|} L(A'), \quad (1)$$

Moreover, the Harsanyi dividend is associated with the Shapley value [48], which adheres to several key axioms: *linearity*, *dummy*, *symmetry* and *efficiency* axioms [48]. This connection provides robust theoretical support for the Harsanyi dividend, enhancing the reliability and trustworthiness of analyses built upon it.

## 3.2. Quantifying the Multimodal Interactions with the Harsanyi Dividend for LVLMS

Based on the definition of the Harsanyi Dividend, we then apply it to quantify multimodal interaction effects on the decoding process in LVLMS.

To begin with, let us clarify the notations used for the decoding process of LVLMS. In LVLMS, an input sample typically includes a prompt  $\mathbf{p}$  and an image  $\mathbf{v}$ . For the token  $\mathbf{y}_t$  at the  $t$ -th step in the generated response  $\mathbf{y}$ , LVLMS utilize information from both  $\mathbf{p}$  and  $\mathbf{v}$ , as well as the previously generated tokens  $\mathbf{y}_{<t}$  to produce the next token. Formally, such a process can be expressed as follows.

$$\begin{aligned} \tilde{P}_t &= \text{SoftMax} [\mathcal{M}_\theta (\mathbf{v}, \mathbf{p}, \mathbf{y}_{<t})], \\ \mathbf{y}_t &= \mathcal{S} (\tilde{P}_t), \end{aligned} \quad (2)$$

where  $\mathcal{M}_\theta (\mathbf{v}, \mathbf{p}, \mathbf{y}_{<t}) \in \mathbb{R}^N$  represents any LVLMS providing logit values. Here  $N$  is the number of candidate tokens in the vocabulary set  $\mathcal{B}$ . Then, in the decoding process of LVLMS, we convert  $\mathcal{M}_\theta (\mathbf{v}, \mathbf{p}, \mathbf{y}_{<t})$  into the probability distribution  $\tilde{P}_t$  using the softmax function and ultimately select the token  $\mathbf{y}_t \in \mathcal{B}$  based on any decoding strategy  $\mathcal{S}$ .

Inspired by previous research [5, 18, 51, 56] for applying the Harsanyi dividend to DNNs, we can analogously consider the inference process of LVLMS as a game  $L(\cdot)$  and deem the input image  $\mathbf{v}$  and the input prompt  $\mathbf{p}$  as players. Thus, we define the whole set of players  $\mathcal{N} = \{\mathbf{v}, \mathbf{p}\}$  and set  $L(\mathcal{N})^{\mathbf{y}_t} = \mathcal{M}_\theta (\mathbf{v}, \mathbf{p}, \mathbf{y}_{<t})^{\mathbf{y}_t}$  representing the logit value for the token  $\mathbf{y}_t$ . In this way, the causal effects of the pattern

Datasets	InstructBLIP [13]	LLaVA-v1.5 [38]	Qwen-VL [3]	mPLUG-owl2 [63]
MME	0.80	0.59	2.10	0.07
CHAIR	0.60	0.06	0.56	0.16

Table 1. **Verifying the existence of interactions through analyzing absolute values of interaction contributions.** Each value represents the average absolute value to all generated tokens. Results reveal that all values are greater than zero, suggesting that interactions participate in the decision-making processes of LVLMs.

$A \subseteq \{\mathbf{v}, \mathbf{p}\}$  on the output token  $\mathbf{y}_t$  can be measured by the Harsanyi dividend as follows,

$$I(A|\{\mathbf{v}, \mathbf{p}\})^{\mathbf{y}_t} = \sum_{A' \subseteq A} (-1)^{|A'| - |A|} L(A')^{\mathbf{y}_t}, \quad (3)$$

Notably, when  $A = \{\mathbf{v}, \mathbf{p}\}$ ,  $I(A|\{\mathbf{v}, \mathbf{p}\})^{\mathbf{y}_t}$  then represents the contribution of multimodal (*i.e.*, image-text) interactions to the sampled token  $\mathbf{y}_t$ .  $A'$  is a subset of  $A$ , which is then any one of the elements in the set  $\{\{\mathbf{v}, \mathbf{p}\}, \{\mathbf{v}\}, \{\mathbf{p}\}, \emptyset\}$ . In parallel, when  $A = \{\mathbf{v}\}$  or  $A = \{\mathbf{p}\}$ ,  $I(A|\{\mathbf{v}, \mathbf{p}\})^{\mathbf{y}_t}$  represents the contribution of each uni-modal information to the sampled token  $\mathbf{y}_t$ .

Based on Equation 3, we then design metrics to thoroughly investigate the roles of multimodal interactions on the LVLm response generation process. For simplicity, we denote  $I(A|\{\mathbf{v}, \mathbf{p}\})^{\mathbf{y}_t}$  as  $I(A)^{\mathbf{y}_t}$  in the following sections.

### 3.3. Verifying the Existence of Interactions

**Insight 1:** LVLms implicitly capture multimodal interactions from input samples and leverage such interactions for decision-making to some extent.

Firstly, we propose to verify whether LVLms already encode multimodal interactions. To this end, we posit that LVLms implicitly utilize such interactions during the decision-making process.

To validate this, we analyze the absolute values of interaction contributions,  $|I(A)^{\mathbf{y}_t}|$ , with  $A = \{\mathbf{v}, \mathbf{p}\}$ . If this value is greater than zero, it indicates that multimodal interactions influence the generation of LVLm responses.

As shown in Table 1, we calculated the mean absolute value of  $|I(A)^{\mathbf{y}_t}|$  across all sampled tokens. Results demonstrate consistent positive values across multiple benchmarks including MME [19] and CHAIR [46]. This empirical evidence confirms that LVLms do implicitly capture image-text interactions during response generation to some extent.

### 3.4. Verifying the Scope of Interactions

**Insight 2:** LVLms exhibit a tendency to primarily apply their understanding of multimodal interactions to the generation of a few key tokens, rather than uniformly across all response tokens.

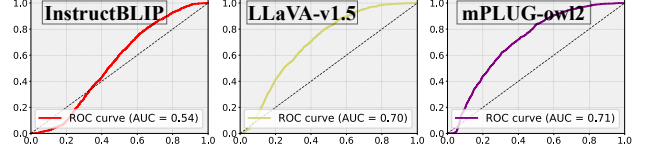


Figure 2. **Verifying the scope of interactions using the Receiver Operating Characteristic (ROC) curve.** Results ( $AUC > 0.5$ ) show that there exists a moderate class separation between keywords tokens and contextual connectives tokens based on the variance of multimodal interactions. These findings suggest that multimodal interactions primarily impact the the generations of keywords in LVLms’ responses.

Based on the results in Section 3.3, we further propose to locate the scope of such interactions in LVLms’ responses. In other words, we expect to analyze how LVLms leverage image-text interactions to formulate responses during the answer-generation phase. Specifically, LVLm-generated answers are typically composed of keywords and contextual connectives. Keywords indicate question-relevant content, while contextual connectives integrate these words and convert them into language expressions. We hypothesize that image-text interactions primarily influence the reasoning process behind keywords generations, shaping the core content of responses.

The key challenge here is to quantitatively measure the involvement of multimodal interactions in the generation of each token. To this end, we propose to utilize the variance of multimodal interaction effects  $\mathcal{D}_{\mathbf{y}_t}(I(A)^{\mathbf{y}_t})$  as a measurement for the level of interaction engagement at the  $t$ -th step. Specifically, when the variance  $\mathcal{D}_{\mathbf{y}_t}(I(A)^{\mathbf{y}_t})$  presents a small value, it indicates that multimodal interactions had almost the same influence on the candidate tokens in the vocabulary for the  $t$ -th step. In other words, multiple candidate tokens exhibit similar  $I(A)^{\mathbf{y}_t}$ , and the model’s token selection becomes interaction-agnostic, implying weak engagement of interactions. By contrast, if  $\mathcal{D}_{\mathbf{y}_t}(I(A)^{\mathbf{y}_t})$  shows a large value, it indicates that multimodal interactions provides meaningful guidance to a few candidate tokens among the whole vocabulary set, implying strong engagement in the token selection. In this way, we hypothesize that the generations of keywords should present higher values of  $\mathcal{D}_{\mathbf{y}_t}(I(A)^{\mathbf{y}_t})$ , compared to contextual connectives.

To validate this, we sample a subset in CHAIR [46] following OPERA [25] and conduct experiments to analyze the differences in  $\mathcal{D}_{\mathbf{y}_t}(I(A)^{\mathbf{y}_t})$  between keywords and contextual connectives in LVLms’ responses. To localize keywords, we tag the part-of-speech of generated words based on spaCy [24]. We argue that nouns typically denote objects, while adjectives, numbers, and adverbs specify the attributes of those objects; verbs and adpositions establish inter-object relationships. Therefore, we regard such words



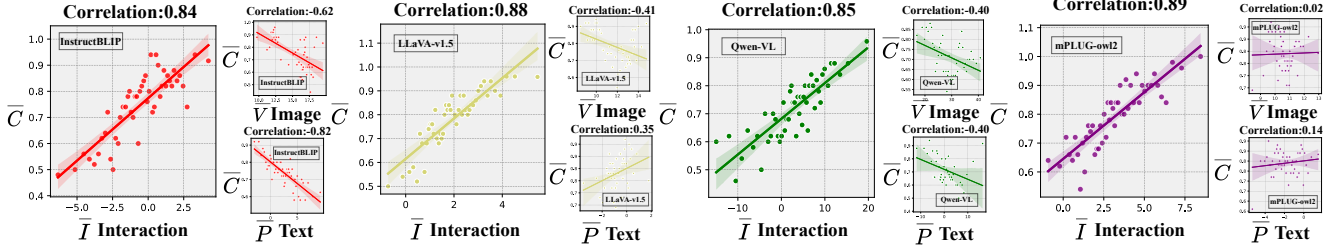


Figure 3. **Verifying the impact of interactions through the Pearson correlation coefficient.** The set of figures for each LVLM illustrates the correlation between the accuracy and the multimodal interaction contributions, the correlation between the accuracy and the visual modality contributions, and the correlation between the accuracy and the textual modality contributions on MME [19] benchmark. Each point corresponds to statistics within a bin  $\mathbf{b}$  of 50 tokens, including the proportion of correct tokens  $\bar{C}_{\mathbf{b}}$ , the average contribution of multimodal interactions  $\bar{I}_{\mathbf{b}}$ , the average contribution of visual modality  $\bar{V}_{\mathbf{b}}$  and the average contribution of textual modality  $\bar{P}_{\mathbf{b}}$ . Results indicate that as the contribution of multimodal interactions increases, the proportion of correct tokens rises, resulting in higher accuracy. Additionally, the influence of multimodal interactions in LVLMs shows a stronger positive correlation with prediction accuracy than that of uni-modal information, indicating that the contribution of multimodal interactions plays a more critical role in ensuring accurate responses.

as keywords and others as contextual connectives. In this way, we treat keywords as positive class instances and construct Receiver Operating Characteristic (ROC) curves by using variance  $\mathcal{D}_{y_t}(I(A)^{y_t})$  as the classification threshold.

As shown in Fig. 2, the Area Under the Curve (AUC) values of various LVLMs exceed 50%. Such results reveal that there exists a moderate class separation between keywords and contextual connectives based on the variance of multimodal interactions  $\mathcal{D}_{y_t}(I(A)^{y_t})$ . This empirical evidence confirms that interactions in LVLMs are primarily focused on the reasoning of keywords tokens, rather than being applied uniformly to the entire autoregressive process.

### 3.5. Verifying the Impact of Interactions

**Insight 3:** The understanding of multimodal interactions in LVLMs positively influences the quality of generated responses, with stronger interactions leading to greater accuracy.

Based on the results in Section 3.4, we expect to further evaluate the impact of multimodal interactions on the generation of keywords tokens. We hypothesize that such multimodal interactions should bring a positive impact on keywords generations, with stronger interactions leading to more accurate responses.

It is challenging to quantify the relationship between the strength of multimodal interactions for keyword tokens and the overall accuracy of the response. To address this, we propose conducting experiments on the MME [19] benchmark for convenient verification. In MME, the keywords in the responses are limited to “yes” or “no”, which are also used to determine the accuracy of the responses. This setup allows us to measure the strength of multimodal interactions for keyword tokens using  $I(A)^{y_t}$ , where  $y_t \in \{yes, no\}$  and  $A = \{\mathbf{v}, \mathbf{p}\}$ , for each response  $r$ . The appearance of the *yes/no* keywords directly indicates the binary correctness of

the response. Furthermore, to better verify the trend of the positive impact of multimodal interactions, we propose to partition all the generated responses on MME into multiple bins based on the value of  $I(A)^{y_t}$  ( $y_t \in \{yes, no\}$ ) sorted in ascending order, with each bin containing  $Q$  samples. Then, we calculate the average contribution of interactions within each bin  $\mathbf{b}$ , denoted by  $\bar{I}_{\mathbf{b}} = \frac{1}{Q} \sum_{r \in \mathbf{b}} I(A)^{y_t}$ . We denote  $\bar{C}_{\mathbf{b}}$  as the ratio of correct responses in each bin  $\mathbf{b}$ . Thus, we can analyze the correlation between  $\bar{I}_{\mathbf{b}}$  and  $\bar{C}_{\mathbf{b}}$  among different bins, allowing us to verify trends in the positive impact of multimodal interactions on response accuracy.

As shown in Fig. 3, we observe a significant monotonic relationship, where higher strength of multimodal interactions corresponds to improved response accuracy. This highlights the effectiveness of multimodal interactions in guiding keyword token selections. To fully complement our analysis for contrast, we also quantified uni-modal contributions on each keyword token  $y_t$  through calculating  $I(\{\mathbf{v}\})^{y_t}$  and  $I(\{\mathbf{p}\})^{y_t}$ . Using the same binning procedure described earlier, we calculated the average contribution of visual modality and textual modality, *i.e.*,  $\bar{V}_{\mathbf{b}} = \frac{1}{Q} \sum_{r \in \mathbf{b}} I(\{\mathbf{v}\})^{y_t}$  and  $\bar{P}_{\mathbf{b}} = \frac{1}{Q} \sum_{r \in \mathbf{b}} I(\{\mathbf{p}\})^{y_t}$  for each bin  $\mathbf{b}$ . In Fig. 3, the correlation of  $\bar{I}$  and  $\bar{C}$ , the correlation of  $\bar{V}$  and  $\bar{C}$ , and the correlation of  $\bar{P}$  and  $\bar{C}$  are compared. Notably, our quantitative analysis demonstrates a more positive correlation between multimodal interactions and response accuracy compared to uni-modal information alone. These findings suggest that image-text interactions plays a more substantial role in generating reliable responses.

## 4. INTER: Interaction Guidance Sampling

Based on the obtained insights, we find that LVLMs exhibit a human-like, though less pronounced, understanding of multimodal interactions, which motivated us to develop efficient methods to reduce hallucinated responses in

**Prompt:** How many uncut fruits are in the image?

$\mathbf{y}_{<t}$  : The number of uncut fruits in image is

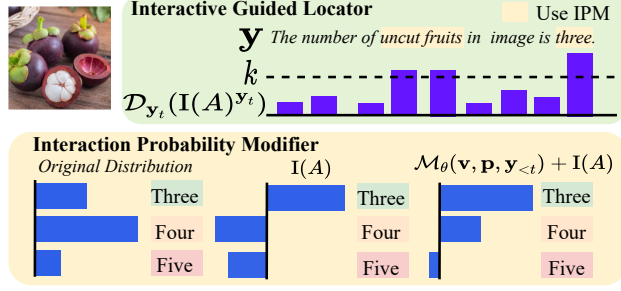


Figure 4. **Overview of INTER.** The Interactive Guided Locator (IGL) uses variance of multimodal interactions to identify keywords of interest. The Interaction Probability Modifier (IPM) uses multimodal interactions to guide the model to sample tokens responsive to visual information related to the question.

LVLMS. To this end, we further propose a simple yet effective method named Interaction Guidance Sampling (INTER). The approach comprises two components: the Interactive Guided Locator and the Interaction Probability Modifier. Specifically, the Interactive Guided Locator is designed to localize keywords in generated responses. Such words typically indicate visual information that is relevant to questions (e.g., objects, object relations, or object attributes). During the keyword generation phase, the Interaction Probability Modifier then guides LVLMS to sample tokens that exhibit stronger reliance on the image-text interactions. Sampling tokens based on the interactions, INTER prevents the interference of the question-irrelevant information, thus reducing the hallucination in LVLMS.

**Interactive Guided Locator.** LVLMS primarily apply the understanding of multimodal interactions to the generation of a few keywords tokens. To this end, we propose the Interactive Guided Locator (IGL) method to indicate such tokens. Following Sec. 3.4, the module calculates the variance of interactions  $\mathcal{D}_{\mathbf{y}_t}(\mathbf{I}(\mathbf{A})^{\mathbf{y}_t})$  at  $t$ -th step during answer synthesis. As shown in Fig. 4, if the variance exceeds the predefined threshold  $k$ , IGL designates  $\beta = \mathbf{1}_{\{\mathcal{D}_{\mathbf{y}_t}(\mathbf{I}(\mathbf{A})^{\mathbf{y}_t}) > k\}}$ , which signifies that the token  $\mathbf{y}_t$  is a keyword in the answer. Conversely, if  $\mathcal{D}_{\mathbf{y}_t}(\mathbf{I}(\mathbf{A})^{\mathbf{y}_t})$  is less than  $k$ , we set  $\beta$  to 0 showing  $\mathbf{y}_t$  is contextual connective.

The Interactive Guided Locator (IGL) localizes keywords in sentences and guides the Modifier only applying interactions enhancement to these tokens. In this way, IGL prevents interference from image-text interactions to contextual connectives, thereby preserving the linguistic coherence of generated answers.

**Interaction Probability Modifier.** The understanding of multimodal interactions in LVLMS positively influences the quality of generated responses. Based on the insight, we present the Interaction Probability Modifier (IPM) to

guide LVLMS sampling tokens. In this way, tokens that are more influenced by image-text interactions are sampled by LVLMS, thereby improving the relevance of answers to multimodal inputs.

Specifically, we utilize Harsanyi dividend [22] to explicitly decouple interactions and treat interactions as prior knowledge to adjust the original logit distribution, as shown in Fig. 4. For each candidate token  $\mathbf{y}_t$ , we can obtain the multimodal interaction contribution  $\mathbf{I}(\mathbf{A})^{\mathbf{y}_t}$  with  $\mathbf{A} = \{\mathbf{v}, \mathbf{p}\}$ , as well as the original logit  $\mathcal{M}_\theta(\mathbf{v}, \mathbf{p}, \mathbf{y}_{<t})^{\mathbf{y}_t}$ . Then, we use  $\mathbf{I}(\mathbf{A}) \in \mathbb{R}^N$  to modify the logit of each candidate token and generate sampling probabilities, formulated as follows:

$$\tilde{P}_t = \text{SoftMax} [\mathcal{M}_\theta(\mathbf{v}, \mathbf{p}, \mathbf{y}_{<t}) + \mathbf{I}(\mathbf{A})]. \quad (4)$$

By doing so, IPM enhances the dependence of LVLMS on multimodal interactions. Therefore, the generation of information unrelated to the input is suppressed, reducing hallucinations in LVLMS.

**Overall Mechanism.** The INTER employs multimodal interaction guidance sampling for keywords, formulated as:

$$\tilde{P}_t = \text{SoftMax} [\mathcal{M}_\theta(\mathbf{v}, \mathbf{p}, \mathbf{y}_{<t}) + \beta \cdot \mathbf{I}(\mathbf{A})], \quad (5)$$

by using a threshold to control  $\beta$  for locating key steps, we help the model focus more on image-text interactions during keywords generations.

## 5. Experiment

In this section, we first describe our experimental settings. Subsequently, we present the model’s performance before and after the application of INTER across various decoding strategies to demonstrate the effectiveness of INTER. Following this, we conduct a parameter analysis and evaluate the performance of INTER across LVLMS with varying parameter scales. Additional results into the performance of INTER can be found in the supplementary materials.

### 5.1. Experimental Settings

**Models.** We conduct experiments on multiple representative LVLMS to demonstrate the generalization ability of INTER. Specifically, our experiments includes the 7B version of Qwen-VL [3], InstructBLIP [13] and mPLUG-owl2 [63], the 7B and 13B versions of LLaVA-v1.5 [38], and 1-26B versions of InternVL2 [9, 10].

**Benchmarks.** To rigorously validate INTER’s enhanced cross-modal comprehension capabilities, we conducted extensive evaluations across Visual Question Answering (VQA) and image captioning tasks. For VQA assessment, we employed four authoritative benchmarks: Polling-based Object Probing Evaluation (POPE) [33] for object hallucination analysis, along with three benchmarks for comprehensive evaluations: MME [19], MM-Bench [39] and MM-Star [7]. The captioning performance was assessed through

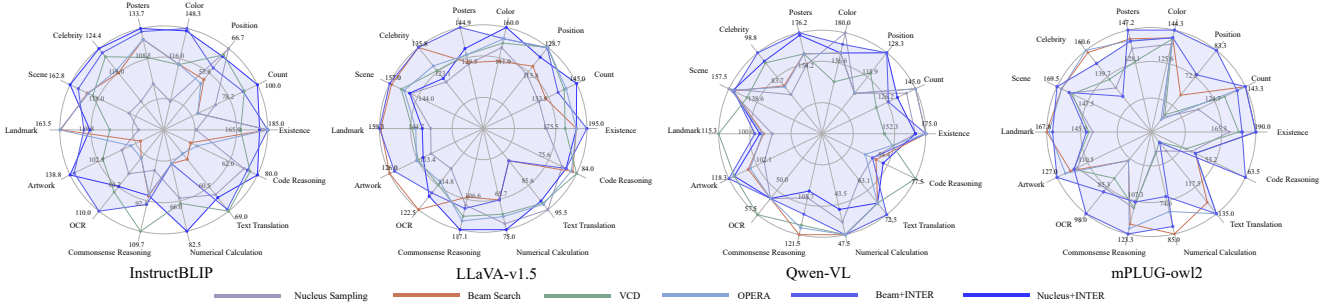


Figure 5. **The scores of 14 subtasks on MME benchmark [19].** The radar charts show that the areas filled in purple are significantly larger, suggesting that using INTER results in noticeable improvements.

Caption Hallucination Assessment with Image Relevance (CHAIR) [46] to quantify object-level hallucination. Additionally, LLaVA-Bench [37] was utilized to analyze hallucinations in open-ended, real-world scenarios. Comprehensive details regarding these benchmarks are provided in the supplementary materials.

**Metrics.** In the POPE [34] benchmark, we implement three question sampling strategies for each dataset, reporting the average F1 score as the primary evaluation metric. Under the MME [19] evaluation, we compute both the total score and perception score, alongside the performance across various subtasks, according to VCD [16]. For the MM-Bench [39] and MMStar [7] benchmarks, we focus on overall performance metrics, while comprehensive analyses of the subtasks are provided in the supplementary materials. Based on OPERA [25], we reported two metrics:  $CHAIR_S(C_S)$  and  $CHAIR_I(C_I)$  on CHAIR [25], which assess the degree of hallucinations at both the sentence and image levels. For the LLaVA-Bench [37] open-ended generation tasks, we use GPT-4o [28] to score a 1-10 scale from two dimensions: semantic accuracy and detail richness.

**Baselines.** We conduct evaluations across five decoding strategies to validate the effectiveness of INTER on hallucination mitigation: Nucleus Sampling [23] ( $p = 1.0$ ), Beam Search [4, 21, 53] ( $N_{beam} = 5$ ), Greedy Search [49] and two state-of-the-art methods VCD\* [16] and OPERA† [25]. \* and † represent correction based on Nucleus Sampling and Beam Search. INTER-enhanced strategies are denoted with ‘+INTER’, which substitute visual inputs of  $\{\mathbf{p}\}$  with random noise while initialize text inputs of  $\{\mathbf{v}\}$  with empty text inputs. All experiments maintain hyperparameters from VCD [16] and OPERA [25] implementations for fair comparisons. Quantitative results represent averages over five runs.

## 5.2. Experimental Results

**Result on POPE [34].** We conducted comparative experiments on POPE to demonstrate the effectiveness of INTER in enhancing LVLMs’ performance on object exist-

tence tasks. As demonstrated in Table 6, INTER achieves consistent improvements across all datasets in POPE, with maximum mean F1-score enhancement reaching 7.5%. Notably, INTER-enhanced Nucleus Sampling outperforms VCD, while ‘Beam+INTER’ surpasses OPERA’s performance. These comparative results validate that emphasizing cross-modal interaction yields superior performance over uni-modal enhancement methods.

**Result on MME [19].** Quantitative analysis through 14 subtasks of MME [19] reveals the task-specific advantages of INTER. As visualized in Fig. 5, our method outperforms baseline methods in most subtasks, particularly excelling in subtasks related to scene text recognition and fine-grained attribute identification. Moreover, INTER demonstrates a 343.7-point absolute improvement in the total score of all 14 subtasks compared to Nucleus Sampling, with more detailed results provided in the supplementary material.

**Result on MM-Bench [39] and MMStar [7].** MM-Bench and MMStar evaluate LVLMs through various subtasks including compositional reasoning and fine-grained perception. As shown in Tab. 7, INTER achieves consistent accuracy improvements across these benchmarks.

**Result on CHAIR [46].** To evaluate INTER’s hallucination mitigation capability in image captioning, we conduct experiments on 500 randomly sampled instances from the CHAIR benchmark with caption lengths 64 and 512 tokens in Tab. 4. Both  $C_S$  and  $C_I$  metrics show lower values indicating reduced hallucinations, where INTER achieves the highest reduction of 34.6% and 18.9% on  $C_S$  and  $C_I$  respectively compared to baseline methods.

## 5.3. Further Analysis

**The Robustness of the Selection of Hyperparameter ( $k$ ).** As shown in Fig. 6, when  $k = 1$ , various LVLMs achieve relatively good performance on different tasks. Furthermore, within the range of  $k \in [0.5, 1.5]$ , the performance of the LVLM remains stable. Such results demonstrate that INTER exhibits robustness to the selection of  $k$ .

**Comparison with Other Methods.** We conducted

Datasets	Order	InstructBLIP [13]		LLaVA-v1.5 [38]		Qwen-VL [3]		mPLUG-owl2 [62]	
		Mean	Range	Mean	Range	Mean	Range	Mean	Range
MME [19]	$I(A \{v, p\})^{y_t}$	0.80	[-9.8, 5.7]	0.59	[-13.8, 5.3]	2.10	[-16.1, 10.0]	0.07	[-20.4, 27.8]
	$I(A \{p, v\})^{y_t}$	4.07	[-7.4, 22.8]	0.59	[-13.8, 9.3]	1.93	[-10.6, 8.2]	0.07	[-16.5, 10.2]
CHAIR [46]	$I(A \{v, p\})^{y_t}$	0.60	[-16.5, 14.2]	0.06	[-3.3, 3.9]	0.56	[-17.8, 12.4]	0.16	[-8.0, 7.7]
	$I(A \{p, v\})^{y_t}$	0.60	[-3.3, 3.9]	0.06	[-3.3, 3.9]	0.94	[-25.4, 8.1]	0.16	[-7.9, 7.5]

Table 2. The range of the metric  $I(A)^{y_t}$ .

model	method	CHAIR (512)		MMStar $\uparrow$	MME $\uparrow$
		$C_S\downarrow$	$C_I\downarrow$		
InstructBLIP [13]	M3ID [17]	63.1	21.1	29.8	1440.6
	Ritual [59]	62.1	20.9	29.5	1576.7
	SID [27]	59.7	21.4	28.1	1385.1
	<b>INTER (ours)</b>	<b>59.0</b>	<b>20.8</b>	<b>30.5</b>	<b>1595.5</b>
LLaVA-v1.5 [38]	M3ID [17]	67.1	19.7	30.9	1322.9
	Ritual [59]	52.4	15.8	31.2	1754.7
	SID [27]	52.0	14.3	31.0	1692.4
	<b>INTER (ours)</b>	<b>51.8</b>	<b>14.1</b>	<b>31.9</b>	<b>1731.6</b>

Table 3. Comparison with other methods.

Max Token	method	InstructBLIP [13]		LLaVA-v1.5 (7B) [38]		mPLUG-owl2 [63]	
		$C_S\downarrow$	$C_I\downarrow$	$C_S\downarrow$	$C_I\downarrow$	$C_S\downarrow$	$C_I\downarrow$
64	○ Nucleus [23]	29.0	15.3	24.4	9.4	26.2	10.9
	● Nucleus+INTER	<b>26.2</b>	<b>10.0</b>	<b>19.8</b>	<b>6.7</b>	<b>24.8</b>	<b>9.4</b>
	○ Beam [4, 21, 53]	21.4	7.2	19.4	6.2	21.6	7.6
	● Beam+INTER	<b>21.0</b>	<b>6.4</b>	<b>17.8</b>	<b>5.9</b>	<b>21.2</b>	<b>7.6</b>
	○ VCD* [16]	33.0	11.8	24.4	8.0	24.0	9.5
	● VCD*+INTER	<b>31.2</b>	<b>11.4</b>	<b>21.0</b>	<b>7.2</b>	<b>21.2</b>	<b>8.3</b>
	○ OPERA $^\dagger$ [25]	19.9	6.8	19.0	6.6	21.0	7.8
	● OPERA $^\dagger$ +INTER	<b>18.4</b>	<b>7.9</b>	<b>19.0</b>	<b>6.3</b>	<b>20.0</b>	<b>7.4</b>
	○ Nucleus [23]	61.0	28.4	54.0	16.1	60.8	20.1
	● Nucleus+INTER	<b>59.0</b>	<b>20.8</b>	<b>51.8</b>	<b>14.1</b>	<b>59.4</b>	<b>19.3</b>
512	○ Beam [4, 21, 53]	55.6	15.8	48.8	13.9	56.4	17.9
	● Beam+INTER	<b>55.4</b>	<b>13.1</b>	<b>46.4</b>	<b>13.4</b>	<b>53.4</b>	<b>17.2</b>
	○ VCD* [16]	58.6	19.2	53.8	16.0	62.8	20.5
	● VCD*+INTER	<b>56.2</b>	<b>18.8</b>	<b>56.0</b>	<b>15.7</b>	<b>60.4</b>	<b>20.5</b>
	○ OPERA $^\dagger$ [25]	48.7	13.5	45.4	13.8	55.2	16.1
	● OPERA $^\dagger$ +INTER	<b>42.2</b>	<b>18.8</b>	<b>47.0</b>	<b>13.6</b>	<b>52.5</b>	<b>15.9</b>

Table 4. **Result on CHAIR [46]**.  $\downarrow$  means that lower values indicate lower hallucination levels.

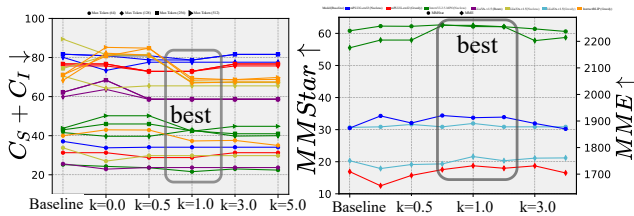


Figure 6. The robustness of the selection of hyperparameter (k).

experiments with M3ID [17], Ritual [59] and SID [27] in Tab. 3. The results demonstrate that our INTER achieves comparable performance among compared methods.

#### Performance on Other Types of Tasks or Different

Models	RefCOCO [64]	
	testA	testB
DeepSeek-VL2-Tiny [60]	87.8	78.4
+INTER	<b>88.6</b>	<b>78.6</b>

Table 5. Performance on other types of tasks or different LVLMS.

**LVLMS.** We conducted experiments with DeepSeek-VL2 [60] on the visual grounding task. As shown in Tab. 5, results show that the INTER boosts the model performance on this task.

**The Range of the Metric  $I(A)^{y_t}$ .** The value range of  $I(A)^{y_t}$  could be influenced by several factors, *e.g.*, benchmarks, LVLMS, etc. These complexities make it challenging to establish a theoretical bound for its value range. Nevertheless, we conducted experiments to empirically assess the distribution of  $I(A)^{y_t}$  in Tab. 2. Moreover, when  $I(A)^{y_t}$  is negative, we consider that such interaction effects may hinder sampling this candidate token, which is considered similarly in prior studies [57, 70].

## 6. Conclusion

In this paper, we confirmed the unexplored phenomenon of the existence, scope, and effects of multimodal interactions in the entire decision-making process of LVLMS. Inspired by this, we propose Interaction Guidance Sampling, a training-free approach that first mitigates hallucinations from the perspective of enhancing the reliance of LVLMS on multimodal interactions. Extensive experiments demonstrate that by reducing the sampling of input-irrelevant information, INTER effectively mitigated hallucinations in the responses of LVLMS. In summary, this research provides a new perspective for mitigating hallucinations in LVLMS, shedding new light on the development of the field.

## References

- [1] Wenbin An, Feng Tian, Sicong Leng, Jiahao Nie, Haonan Lin, QianYing Wang, Guang Dai, Ping Chen, and Shijian Lu. Agla: Mitigating object hallucinations in large vision-language models with assembly of global and local attention. *arXiv preprint arXiv:2406.12718*, 2024. 2, 3
- [2] Jinze Bai, Shuai Bai, Yunfei Chu, Zeyu Cui, Kai Dang, Xiaodong Deng, Yang Fan, Wenbin Ge, Yu Han, Fei



- Huang, et al. Qwen technical report. *arXiv preprint arXiv:2309.16609*, 2023. 2
- [3] Jinze Bai, Shuai Bai, Shusheng Yang, Shijie Wang, Sinan Tan, Peng Wang, Junyang Lin, Chang Zhou, and Jingren Zhou. Qwen-vl: A frontier large vision-language model with versatile abilities. *arXiv preprint arXiv:2308.12966*, 2023. 1, 2, 4, 6, 8, 13, 14, 15, 20
- [4] Nicolas Boulanger-Lewandowski, Yoshua Bengio, and Pascal Vincent. Audio chord recognition with recurrent neural networks. In *ISMIR*, pages 335–340. Curitiba, 2013. 7, 8, 12, 13, 14, 15, 19, 21, 22, 23
- [5] Hugh Chen, Scott M Lundberg, and Su-In Lee. Explaining a series of models by propagating shapley values. *Nature communications*, 13(1):4512, 2022. 3
- [6] Lu Chen, Siyu Lou, Keyan Zhang, Jin Huang, and Quanshi Zhang. Harsanyinet: Computing accurate shapley values in a single forward propagation. *arXiv preprint arXiv:2304.01811*, 2023. 3
- [7] Lin Chen, Jinsong Li, Xiaoyi Dong, Pan Zhang, Yuhang Zang, Zehui Chen, Haodong Duan, Jiaqi Wang, Yu Qiao, Dahua Lin, et al. Are we on the right way for evaluating large vision-language models? *arXiv preprint arXiv:2403.20330*, 2024. 2, 6, 7, 12, 13, 19, 22, 23
- [8] Zhiyang Chen, Yousong Zhu, Yufei Zhan, Zhaowen Li, Chaoyang Zhao, Jinqiao Wang, and Ming Tang. Mitigating hallucination in visual language models with visual supervision. *arXiv preprint arXiv:2311.16479*, 2023. 1, 2
- [9] Zhe Chen, Weiyun Wang, Hao Tian, Shenglong Ye, Zhangwei Gao, Erfei Cui, Wenwen Tong, Kongzhi Hu, Jiapeng Luo, Zheng Ma, et al. How far are we to gpt-4v? closing the gap to commercial multimodal models with open-source suites. *arXiv preprint arXiv:2404.16821*, 2024. 2, 6, 14
- [10] Zhe Chen, Jiannan Wu, Wenhai Wang, Weijie Su, Guo Chen, Sen Xing, Muyan Zhong, Qinglong Zhang, Xizhou Zhu, Lewei Lu, et al. Internvl: Scaling up vision foundation models and aligning for generic visual-linguistic tasks. In *Proceedings of the IEEE/CVF Conference on Computer Vision and Pattern Recognition*, pages 24185–24198, 2024. 1, 2, 6, 12, 13, 14
- [11] Zhaorun Chen, Zhuokai Zhao, Hongyin Luo, Huaxiu Yao, Bo Li, and Jiawei Zhou. Halc: Object hallucination reduction via adaptive focal-contrast decoding. *arXiv preprint arXiv:2403.00425*, 2024. 1, 2, 3
- [12] Wei-Lin Chiang, Zhuohan Li, Zi Lin, Ying Sheng, Zhanghao Wu, Hao Zhang, Lianmin Zheng, Siyuan Zhuang, Yonghao Zhuang, Joseph E Gonzalez, et al. Vicuna: An open-source chatbot impressing gpt-4 with 90%\* chatgpt quality. See <https://vicuna.lmsys.org> (accessed 14 April 2023), 2(3):6, 2023. 2
- [13] Wenliang Dai, Junnan Li, Dongxu Li, Anthony Meng Huat Tiong, Junqi Zhao, Weisheng Wang, Boyang Li, Pascale Fung, and Steven Hoi. Instructblip: Towards general-purpose vision-language models with instruction tuning, 2023. 1, 2, 4, 6, 8, 13, 14, 15, 20
- [14] Huiqi Deng, Qihan Ren, Hao Zhang, and Quanshi Zhang. Discovering and explaining the representation bottleneck of dnns. *arXiv preprint arXiv:2111.06236*, 2021. 3
- [15] Shichao Dong, Jin Wang, Jiajun Liang, Haoqiang Fan, and Renhe Ji. Explaining deepfake detection by analysing image matching. In *European Conference on Computer Vision*, pages 18–35. Springer, 2022. 3
- [16] Leng et al. Mitigating object hallucinations in large vision-language models through visual contrastive decoding. *arXiv preprint arXiv:2311.16922*, 2023. 1, 2, 3, 7, 8, 12, 13, 14, 15, 19, 21, 22, 23
- [17] Alessandro Favero, Luca Zancato, Matthew Trager, Siddharth Choudhary, Pramuditha Perera, Alessandro Achille, Ashwin Swaminathan, and Stefano Soatto. Multi-modal hallucination control by visual information grounding. In *Proceedings of the IEEE/CVF Conference on Computer Vision and Pattern Recognition*, pages 14303–14312, 2024. 2, 3, 8
- [18] Daniel Fryer, Inga Strümke, and Hien Nguyen. Shapley values for feature selection: The good, the bad, and the axioms. *Ieee Access*, 9:144352–144360, 2021. 3
- [19] Chaoyou Fu, Peixian Chen, Yunhang Shen, Yulei Qin, Mengdan Zhang, Xu Lin, Zhenyu Qiu, Wei Lin, Jinrui Yang, Xianwu Zheng, et al. Mme: A comprehensive evaluation benchmark for multimodal large language models. *arXiv preprint arXiv:2306.13394*, 2023. 2, 4, 5, 6, 7, 8, 12, 13, 14, 15
- [20] Michel Grabisch and Marc Roubens. An axiomatic approach to the concept of interaction among players in cooperative games. *International Journal of game theory*, 28(4):547–565, 1999. 3
- [21] Alex Graves. Sequence transduction with recurrent neural networks. *arXiv preprint arXiv:1211.3711*, 2012. 7, 8, 12, 13, 14, 15, 19, 21, 22, 23
- [22] John C Harsanyi and John C Harsanyi. A simplified bargaining model for the n-person cooperative game. *Papers in game theory*, pages 44–70, 1982. 2, 3, 6
- [23] Ari Holtzman, Jan Buys, Li Du, Maxwell Forbes, and Yejin Choi. The curious case of neural text degeneration. In *International Conference on Learning Representations*, 2019. 7, 8, 13, 14, 15, 19, 21, 22, 23
- [24] Matthew Honnibal. spacy 2: Natural language understanding with bloom embeddings, convolutional neural networks and incremental parsing. (*No Title*), 2017. 4
- [25] Qidong Huang, Xiaoyi Dong, Pan Zhang, Bin Wang, Conghui He, Jiaqi Wang, Dahua Lin, Weiming Zhang, and Nenghai Yu. Opera: Alleviating hallucination in multimodal large language models via over-trust penalty and retrospection-allocation. In *Proceedings of the IEEE/CVF Conference on Computer Vision and Pattern Recognition*, pages 13418–13427, 2024. 1, 2, 3, 4, 7, 8, 12, 13, 14, 15, 19, 21, 22, 23
- [26] Drew A Hudson and Christopher D Manning. Gqa: A new dataset for real-world visual reasoning and compositional question answering. In *Proceedings of the IEEE/CVF conference on computer vision and pattern recognition*, pages 6700–6709, 2019. 12, 14
- [27] Fushuo Huo, Wenchao Xu, Zhong Zhang, Haozhao Wang, Zhicheng Chen, and Peilin Zhao. Self-introspective decoding: Alleviating hallucinations for large vision-language models. *arXiv preprint arXiv:2408.02032*, 2024. 3, 8

- [28] Aaron Hurst, Adam Lerer, Adam P Goucher, Adam Perelman, Aditya Ramesh, Aidan Clark, AJ Ostrow, Akila Welihinda, Alan Hayes, Alec Radford, et al. Gpt-4o system card. *arXiv preprint arXiv:2410.21276*, 2024. 7, 14, 15
- [29] Jitesh Jain, Jianwei Yang, and Humphrey Shi. Vcoder: Versatile vision encoders for multimodal large language models. In *Proceedings of the IEEE/CVF Conference on Computer Vision and Pattern Recognition*, pages 27992–28002, 2024. 1
- [30] Chaoya Jiang, Haiyang Xu, Mengfan Dong, Jiaying Chen, Wei Ye, Ming Yan, Qinghao Ye, Ji Zhang, Fei Huang, and Shikun Zhang. Hallucination augmented contrastive learning for multimodal large language model. In *Proceedings of the IEEE/CVF Conference on Computer Vision and Pattern Recognition*, pages 27036–27046, 2024. 1, 2
- [31] Chenliang Li, Haiyang Xu, Junfeng Tian, Wei Wang, Ming Yan, Bin Bi, Jiabo Ye, Hehong Chen, Guohai Xu, Zheng Cao, et al. mplug: Effective and efficient vision-language learning by cross-modal skip-connections. *arXiv preprint arXiv:2205.12005*, 2022. 1
- [32] Xiang Lisa Li, Ari Holtzman, Daniel Fried, Percy Liang, Jason Eisner, Tatsunori Hashimoto, Luke Zettlemoyer, and Mike Lewis. Contrastive decoding: Open-ended text generation as optimization. *arXiv preprint arXiv:2210.15097*, 2022. 3
- [33] Yifan Li, Yifan Du, Kun Zhou, Jinpeng Wang, Wayne Xin Zhao, and Ji-Rong Wen. Evaluating object hallucination in large vision-language models. *arXiv preprint arXiv:2305.10355*, 2023. 2, 6, 12
- [34] Yifan Li, Yifan Du, Kun Zhou, Jinpeng Wang, Wayne Xin Zhao, and Ji-Rong Wen. Evaluating object hallucination in large vision-language models. *arXiv preprint arXiv:2305.10355*, 2023. 7, 13, 20
- [35] Tsung-Yi Lin, Michael Maire, Serge Belongie, James Hays, Pietro Perona, Deva Ramanan, Piotr Dollár, and C Lawrence Zitnick. Microsoft coco: Common objects in context. In *Computer Vision–ECCV 2014: 13th European Conference, Zurich, Switzerland, September 6–12, 2014, Proceedings, Part V 13*, pages 740–755. Springer, 2014. 12, 13, 14, 20
- [36] Fuxiao Liu, Kevin Lin, Linjie Li, Jianfeng Wang, Yaser Yacoob, and Lijuan Wang. Mitigating hallucination in large multi-modal models via robust instruction tuning. *arXiv preprint arXiv:2306.14565*, 2023. 1
- [37] Haotian Liu. Llava-bench in the wild dataset. <https://huggingface.co/datasets/liuhaotian/llava-bench-in-the-wild>. Accessed: 2025-02-20. 2, 7, 13, 15
- [38] Haotian Liu, Chunyuan Li, Yuheng Li, and Yong Jae Lee. Improved baselines with visual instruction tuning, 2023. 1, 2, 4, 6, 8, 13, 14, 15, 19, 20, 21, 22
- [39] Yuan Liu, Haodong Duan, Yuanhan Zhang, Bo Li, Songyang Zhang, Wangbo Zhao, Yike Yuan, Jiaqi Wang, Conghui He, Ziwei Liu, Kai Chen, and Dahua Lin. Mmbench: Is your multi-modal model an all-around player? *arXiv preprint arXiv:2307.06281*, 2023. 2, 6, 7, 12, 13, 19, 21, 22
- [40] Yeji Park, Deokyeong Lee, Junsuk Choe, and Buru Chang. Convis: Contrastive decoding with hallucination visualization for mitigating hallucinations in multimodal large language models. *arXiv preprint arXiv:2408.13906*, 2024. 2, 3
- [41] Suzanne Petryk, David M Chan, Anish Kachinthaya, Haodi Zou, John Canny, Joseph E Gonzalez, and Trevor Darrell. Aloha: A new measure for hallucination in captioning models. *arXiv preprint arXiv:2404.02904*, 2024. 2
- [42] Xiaoye Qu, Jiashuo Sun, Wei Wei, and Yu Cheng. Look, compare, decide: Alleviating hallucination in large vision-language models via multi-view multi-path reasoning. *arXiv preprint arXiv:2408.17150*, 2024. 2, 3
- [43] Jie Ren, Die Zhang, Yisen Wang, Lu Chen, Zhanpeng Zhou, Yiting Chen, Xu Cheng, Xin Wang, Meng Zhou, Jie Shi, et al. A unified game-theoretic interpretation of adversarial robustness. *arXiv preprint arXiv:2111.03536*, 4, 2021. 3
- [44] Jie Ren, Zhanpeng Zhou, Qirui Chen, and Quanshi Zhang. Can we faithfully represent masked states to compute shapley values on a dnn? *arXiv preprint arXiv:2105.10719*, 2021. 2
- [45] Jie Ren, Mingjie Li, Qirui Chen, Huiqi Deng, and Quanshi Zhang. Defining and quantifying the emergence of sparse concepts in dnns. In *Proceedings of the IEEE/CVF conference on computer vision and pattern recognition*, pages 20280–20289, 2023. 2
- [46] Anna Rohrbach, Lisa Anne Hendricks, Kaylee Burns, Trevor Darrell, and Kate Saenko. Object hallucination in image captioning. In *Proceedings of the 2018 Conference on Empirical Methods in Natural Language Processing*, pages 4035–4045, 2018. 2, 4, 7, 8, 12, 13, 20
- [47] Dustin Schwenk, Apoorv Khandelwal, Christopher Clark, Kenneth Marino, and Roozbeh Mottaghi. A-okvqa: A benchmark for visual question answering using world knowledge. In *European Conference on Computer Vision*, pages 146–162. Springer, 2022. 12, 13, 14, 20
- [48] Lloyd S Shapley. A value for n-person games. *Contribution to the Theory of Games*, 2, 1953. 2, 3
- [49] Yifan Song, Guoyin Wang, Sujian Li, and Bill Yuchen Lin. The good, the bad, and the greedy: Evaluation of llms should not ignore non-determinism. *arXiv preprint arXiv:2407.10457*, 2024. 7, 14, 15, 19, 20, 21, 22, 23
- [50] Zhiqing Sun, Sheng Shen, Shengcao Cao, Haotian Liu, Chunyuan Li, Yikang Shen, Chuang Gan, Liang-Yan Gui, Yu-Xiong Wang, Yiming Yang, et al. Aligning large multi-modal models with factually augmented rlhf. *arXiv preprint arXiv:2309.14525*, 2023. 1, 2
- [51] Mukund Sundararajan and Amir Najmi. The many shapley values for model explanation. In *International conference on machine learning*, pages 9269–9278. PMLR, 2020. 3
- [52] Mukund Sundararajan, Kedar Dhamdhere, and Ashish Agarwal. The shapley taylor interaction index. In *International conference on machine learning*, pages 9259–9268. PMLR, 2020. 3
- [53] Ilya Sutskever, Oriol Vinyals, and Quoc V Le. Sequence to sequence learning with neural networks. *Advances in neural information processing systems*, 27, 2014. 7, 8, 12, 13, 14, 15, 19, 21, 22, 23
- [54] Hugo Touvron, Louis Martin, Kevin Stone, Peter Albert, Amjad Almahairi, Yasmine Babaei, Nikolay Bashlykov,

- Soumya Batra, Prajjwal Bhargava, Shruti Bhosale, et al. Llama 2: Open foundation and fine-tuned chat models. *arXiv preprint arXiv:2307.09288*, 2023. 2
- [55] Junyang Wang, Yuhang Wang, Guohai Xu, Jing Zhang, Yukai Gu, Haitao Jia, Ming Yan, Ji Zhang, and Jitao Sang. An llm-free multi-dimensional benchmark for mlms hallucination evaluation. *arXiv preprint arXiv:2311.07397*, 2023. 1, 2
- [56] Jin Wang, Shichao Dong, Yapeng Zhu, Kelu Yao, Weidong Zhao, Chao Li, and Ping Luo. Diagnosing the compositional knowledge of vision language models from a game-theoretic view. *arXiv preprint arXiv:2405.17201*, 2024. 2, 3
- [57] Xin Wang, Jie Ren, Shuyun Lin, Xiangming Zhu, Yisen Wang, and Quanshi Zhang. A unified approach to interpreting and boosting adversarial transferability. In *International Conference on Learning Representations*, 2020. 3, 8
- [58] Xin Wang, Shuyun Lin, Hao Zhang, Yufei Zhu, and Quanshi Zhang. Interpreting attributions and interactions of adversarial attacks. In *Proceedings of the IEEE/CVF International Conference on Computer Vision*, pages 1095–1104, 2021. 3
- [59] Sangmin Woo, Jaehyuk Jang, Donguk Kim, Yubin Choi, and Changick Kim. Ritual: Random image transformations as a universal anti-hallucination lever in lvlms. *arXiv preprint arXiv:2405.17821*, 2024. 8
- [60] Zhiyu Wu, Xiaokang Chen, Zizheng Pan, Xingchao Liu, Wen Liu, Damai Dai, Huazuo Gao, Yiyang Ma, Chengyue Wu, Bingxuan Wang, et al. Deepseek-vl2: Mixture-of-experts vision-language models for advanced multimodal understanding. *arXiv preprint arXiv:2412.10302*, 2024. 8
- [61] Kelu Yao, Jin Wang, Boyu Diao, and Chao Li. Towards understanding the generalization of deepfake detectors from a game-theoretical view. In *Proceedings of the IEEE/CVF International Conference on Computer Vision*, pages 2031–2041, 2023. 3
- [62] Qinghao Ye, Haiyang Xu, Guohai Xu, Jiabo Ye, Ming Yan, Yiyang Zhou, Junyang Wang, Anwen Hu, Pengcheng Shi, Yaya Shi, Chenliang Li, Yuanhong Xu, Hehong Chen, Junfeng Tian, Qian Qi, Ji Zhang, and Fei Huang. mplug-owl: Modularization empowers large language models with multimodality. *arXiv preprint arXiv:2304.14178*, 2023. 8
- [63] Qinghao Ye, Haiyang Xu, Jiabo Ye, Ming Yan, Anwen Hu, Haowei Liu, Qi Qian, Ji Zhang, and Fei Huang. mplug-owl2: Revolutionizing multi-modal large language model with modality collaboration. In *Proceedings of the IEEE/CVF Conference on Computer Vision and Pattern Recognition*, pages 13040–13051, 2024. 1, 2, 4, 6, 8, 13, 14, 15, 19, 20, 21, 22, 23
- [64] Licheng Yu, Patrick Poirson, Shan Yang, Alexander C Berg, and Tamara L Berg. Modeling context in referring expressions. In *Computer Vision—ECCV 2016: 14th European Conference, Amsterdam, The Netherlands, October 11–14, 2016, Proceedings, Part II 14*, pages 69–85. Springer, 2016. 8
- [65] Qifan Yu, Juncheng Li, Longhui Wei, Liang Pang, Wentao Ye, Bosheng Qin, Siliang Tang, Qi Tian, and Yueting Zhuang. Hallucidoctor: Mitigating hallucinatory toxicity in visual instruction data. In *Proceedings of the IEEE/CVF Conference on Computer Vision and Pattern Recognition*, pages 12944–12953, 2024. 1
- [66] Zihao Yue, Liang Zhang, and Qin Jin. Less is more: Mitigating multimodal hallucination from an eos decision perspective. *arXiv preprint arXiv:2402.14545*, 2024.
- [67] Bohan Zhai, Shijia Yang, Chenfeng Xu, Sheng Shen, Kurt Keutzer, and Manling Li. Halle-switch: Controlling object hallucination in large vision language models. *arXiv e-prints*, pages arXiv–2310, 2023. 1
- [68] Die Zhang, Hao Zhang, Huilin Zhou, Xiaoyi Bao, Da Huo, Ruizhao Chen, Xu Cheng, Mengyue Wu, and Quanshi Zhang. Building interpretable interaction trees for deep nlp models. In *Proceedings of the AAAI Conference on Artificial Intelligence*, pages 14328–14337, 2021. 3
- [69] Hao Zhang, Xu Cheng, Yiting Chen, and Quanshi Zhang. Game-theoretic interactions of different orders. *arXiv preprint arXiv:2010.14978*, 2020. 3
- [70] Hao Zhang, Yichen Xie, Longjie Zheng, Die Zhang, and Quanshi Zhang. Interpreting multivariate shapley interactions in dnns. In *Proceedings of the AAAI Conference on Artificial Intelligence*, pages 10877–10886, 2021. 3, 8
- [71] Huilin Zhou, Hao Zhang, Huiqi Deng, Dongrui Liu, Wen Shen, Shih-Han Chan, and Quanshi Zhang. Explaining generalization power of a dnn using interactive concepts. In *AAAI Conference on Artificial Intelligence*, 2023. 3
- [72] Xin Zou, Yizhou Wang, Yibo Yan, Sirui Huang, Kening Zheng, Junkai Chen, Chang Tang, and Xuming Hu. Look twice before you answer: Memory-space visual retracing for hallucination mitigation in multimodal large language models. *arXiv preprint arXiv:2410.03577*, 2024. 2, 3

## 7. Details of the Benchmarks

**POPE.** The Polling-based Object Probing Evaluation (POPE) [33] utilizes images sampled from several datasets, including MSCOCO [35], A-OKVQA [47], and GQA [26]. Every question in POPE is *"Is there a <object> in the image?"*. For each dataset, it incorporates random, popular, and adversarial question sampling strategies to sample <object> and create three partitions. Random represents randomly selecting an object from the candidate object set. Popular means selecting the objects that occur more frequently. Adversarial refers to select objects that have a high co-occurrence frequency with the objects in the image. Therefore, the adversarial partition is the most challenging, as hallucinations are often caused by a high co-occurrence frequency between objects.

**MME.** MME [19] evaluates LVLMs using 14 subtasks from the perspectives of perception and cognition. There are four subtasks for the evaluation of the cognition ability, including commonsense reasoning, numerical calculation, text translation, and code reasoning. The remaining subtasks are used to evaluate perceptual abilities from the perspectives of coarse grained recognition, fine grained recognition, and OCR. Each image corresponds to two questions with opposing answers. For each subtask, the score of LVLMs is represented by the proportion of all questions answered correctly, as well as the proportion of both questions for each image answered correctly.

**MM-Bench.** MM-Bench [39] employs 20 subtasks to evaluate LVLMs in detail. These 20 subtasks are further divided into six perspectives: 'Coarse Perception (CP)', 'Cross-instance Fine-grained Perception (FP-C)', 'Single-instance Fine-grained Perception (FP-S)', 'Attribute Reasoning (AR)', 'Logic Reasoning (LR)', and 'Relation Reasoning (RR)'. For each sample, MM-Bench sets several options and requires the LVLMs to return one of them. The template for each question is *'Answer with the option's letter from the given choices directly.'* More importantly, MM-Bench creates questions with the same content but differing option sequences by repeatedly rotating the order of them. Then, for each sample, the accuracy across all orders is collected, and if all are answered correctly, the LVLMs score for that sample. Therefore, MM-Bench's evaluation of LVLMs is more rigorous and is not influenced by the order of the options.

**MMStar.** Like MM-Bench, MMStar [7] also establishes multiple subtasks and categorizes them into six perspectives: 'Coarse Perception (CP)', 'Fine-Grained Perception (FP)', 'Instance Reasoning (IR)', 'Logical Reasoning (LR)', 'Science & Technology (ST)' and 'Math (MA)'. Every aspect have three subtasks. But the difference is that MMStar uses a four-tier filtering mechanism to select 1,500 elite samples from an initial pool of 22,401 samples. Each sample strictly adheres to three criteria during the filter-

ing process: it must rely on visual content comprehension, cover a broad range of ability dimensions, and require advanced multimodal reasoning capabilities. Therefore, using MMStar for evaluation can better reflect the capabilities of LVLMs.

**CHAIR.** CHAIR [46] has established two metrics,  $CHAIR_S$  and  $CHAIR_I$ , to assess the degree of hallucination in the generated responses. Where  $CHAIR_S = \frac{|\{captions\ with\ hallucinated\ objects\}|}{|\{all\ captions\}|}$  indicates the degree of hallucination at the sentence level, while  $CHAIR_I = \frac{|\{hallucinated\ objects\}|}{|\{all\ mentioned\ objects\}|}$  represents the degree of hallucination at the object level. Following previous work, we randomly sampled 500 samples and used *'Please describe this image in detail.'* to guide the LVLMs in generating captions for the images.

## 8. Result on InternVL2.5-MPO

In order to further demonstrate the effectiveness of INTER, we conducted a comparison on the current state-of-the-art LVLm InternVL2.5-MPO (8B) [10]. As shown in Tab. 8, the performance of INTER is superior to the baseline methods across various benchmarks. Moreover, 'Nucleus+INTER' performs better than VCD [16] across all benchmarks, while 'Beam+INTER' also performs better than OPERA [25].

## 9. Ablation Study on Interaction Guide Locator.

In addition to the effectiveness analysis of the Interaction Guide Locator based on Beam Search [4, 21, 53], we also conducted ablation experiments on various decoding strategies for IGL. As shown in Tab. 9, we evaluated the performance improvement brought by IGL on MME [19]. It can be observed that the performance significantly decreases without IGL across all decoding strategies, suggesting that IGL identifies the positions of keywords, preventing the excessive guidance of interactions, thereby effectively improving performance.

## 10. Parameter Analysis of Interaction Guide Locator.

Through experiments on CHAIR [46] and MME [19] benchmarks, we analyze how the interaction guidance coefficient  $k$  affects the performance of INTER.

As shown in Fig. 7, varying  $k$  values lead to significantly different behaviors in LLaVA-v1.5. When  $k = 0.0$  which applies the Interaction Probability Modifier at all decoding steps, we observe reduced hallucination for short sequences after using INTER. However, this approach harms performance in longer sequences due to unnecessary modifica-



method	InstructBLIP [13]		LLaVA-v1.5 (7B) [38]		Qwen-VL [3]		mPLUG-owl2 [63]	
	COCO [35]	AOKVQA [47]	COCO [35]	AOKVQA [47]	COCO [35]	AOKVQA [47]	COCO [35]	AOKVQA [47]
○ Nucleus [23]	80.1	78.5	79.7	79.1	81.7	83.2	80.4	78.0
● Nucleus+INTER	83.3 (↑3.2)	82.4 (↑3.9)	85.7 (↑6.0)	82.6 (↑3.5)	86.2 (↑4.5)	86.1 (↑2.9)	81.9 (↑1.5)	79.1 (↑1.1)
○ Beam [4, 21, 53]	81.9	81.1	84.9	84.3	83.4	85.0	83.3	82.3
● Beam+INTER	84.6 (↑2.7)	83.6 (↑2.5)	85.5 (↑0.6)	84.9 (↑0.6)	86.1 (↑2.7)	86.4 (↑1.4)	83.7 (↑0.4)	82.3 (↑0.0)
○ VCD* [16]	81.4	81.0	84.5	82.3	86.0	86.4	82.3	79.2
● VCD*+INTER	82.9 (↑1.5)	80.8 (↓0.2)	85.6 (↑1.1)	83.0 (↑0.7)	86.3 (↑0.3)	86.4 (↑0.0)	82.8 (↑0.5)	79.3 (↑0.1)
○ OPERA <sup>†</sup> [25]	84.7	83.7	85.3	84.1	83.4	85.1	83.4	82.1
● OPERA <sup>†</sup> +INTER	85.2 (↑0.5)	85.0 (↑1.3)	85.8 (↑0.5)	84.8 (↑0.7)	83.5 (↑0.1)	84.4 (↓0.7)	83.4 (↑0.0)	82.3 (↑0.2)

Table 6. **The average F1-score on the POPE benchmark [34].** ↑ means that higher values indicate lower hallucination levels. The results indicate that applying INTER calibration, the models showed a reduction in hallucinations.

model	benchmark	Nucleus	Nucleus+INTER	Beam	Beam+INTER	VCD*	VCD*+INTER	OPERA <sup>†</sup>	OPERA <sup>†</sup> +INTER
LLaVA-v1.5 (7B) [38]	MM-Bench [39] ↑	57.3	<b>62.6</b>	65.1	<b>65.1</b>	62.5	<b>62.9</b>	65.0	<b>65.0</b>
	MMStar [7] ↑	29.3	<b>31.9</b>	31.1	<b>31.7</b>	30.3	<b>31.1</b>	31.4	<b>32.9</b>
mPLUG-owl2 [63]	MM-Bench [39] ↑	57.0	<b>61.4</b>	63.5	<b>63.7</b>	59.2	<b>59.5</b>	63.4	<b>63.6</b>
	MMStar [7] ↑	30.5	<b>32.3</b>	30.7	<b>30.5</b>	31.5	<b>32.3</b>	30.5	<b>30.9</b>

Table 7. **Validation of INTER on MM-Bench [39] and MMStar [7].** ↑ means that higher values indicate lower hallucination levels.

model	benchmark	Nucleus	Nucleus+INTER	Beam	Beam+INTER	VCD*	VCD*+INTER	OPERA <sup>†</sup>
InternVL2.5-MPO (8B) [38]	MME (Total Score) [19] ↑	2175.7	<b>2204.8</b>	2298.3	<b>2316.4</b>	2189.2	<b>2209.9</b>	2299.7
	POPE (MSCOCO) [34] ↑	85.7	<b>89.2</b>	88.7	<b>89.3</b>	88.6	88.5	88.9
	MM-Bench [39] ↑	80.1	<b>81.5</b>	84.4	<b>84.6</b>	80.8	<b>81.6</b>	84.4
	MMStar [7] ↑	60.8	<b>62.5</b>	63.0	<b>63.9</b>	61.9	<b>63.3</b>	63.5
	CHAIR ( $C_S+C_I$ ) [46] ↓	25.2	<b>21.6</b>	23.6	<b>19.7</b>	25.5	25.9	22.0
	LLaVA-Bench [37] ↑	9.5	<b>11.9</b>	9.3	<b>12.5</b>	10.1	<b>11.2</b>	10.5

Table 8. **Validation of INTER on the state-of-the-art LVLm InternVL2.5-MPO [10].** \* and † represent correction based on Nucleus Sampling and Beam Search.

method	InstructBLIP [13]	LLaVA-v1.5 [38]	mPLUG-owl2 [63]
○ Nucleus+IPM	1569.7	1690.9	1640.6
● Nucleus+INTER	<b>1595.5</b>	<b>1731.6</b>	<b>1641.7</b>
○ Beam+IPM	1556.2	1648.6	1623.0
● Beam+INTER	<b>1562.2</b>	<b>1744.0</b>	<b>1716.1</b>
○ VCD*+IPM	1583.6	1700.0	1620.1
● VCD*+INTER	<b>1605.0</b>	<b>1749.6</b>	<b>1626.2</b>
○ OPERA <sup>†</sup> +IPM	1553.5	1720.8	1625.7
● OPERA <sup>†</sup> +INTER	<b>1567.0</b>	<b>1727.4</b>	<b>1741.7</b>

Table 9. **Ablation Study on Interaction Guide Locator (IGL).**

tions at non-critical positions, as evidenced by the performance drop compared to  $k = 1.0$ .

Fig. 8 reveals model-dependent optimal  $k$  values. On MME, InstructBLIP achieves peak performance at  $k = 1.3$ , beyond which excessive adjustment suppression causes gradual performance degradation. This suggests a balance between necessary corrections and interference avoidance. Based on these findings, we set  $k = 1.3$  for InstructBLIP and  $k = 1.0$  for other LVLms in all experiments.

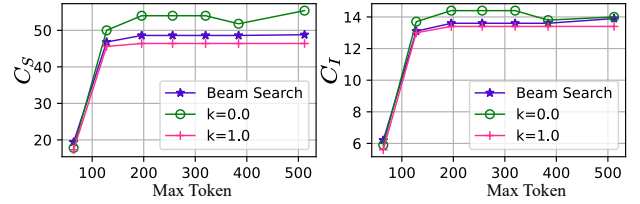


Figure 7. **Parameter analysis of  $k$  in Interaction Guide Locator.** Evaluation of  $C_I$  and  $C_S$  after using different  $k$  to guide Beam Search [4, 21, 53] on various lengths on CHAIR [46].

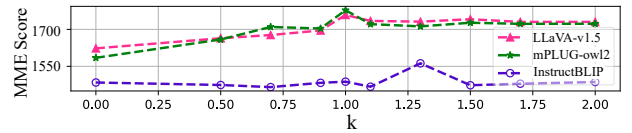


Figure 8. **Parameter analysis of  $k$  on MME [19].** Each value represents total score of using INTER on Beam Search [4, 21, 53].

method	InternVL2 [9, 10]				LLaVA-v1.5 [38]	
	1B	4B	8B	26B	7B	13B
○ Nucleus [23]	1689.0	1914.7	2040.9	1950.3	1502.2	1637.2
● Nucleus+INTER	<b>1721.6</b>	<b>1985.1</b>	<b>2131.5</b>	<b>2047.0</b>	<b>1731.6</b>	<b>1690.3</b>
○ Beam [4, 21, 53]	1715.8	2074.3	2145.8	2219.0	1707.2	1760.5
● Beam+INTER	<b>1743.1</b>	<b>2075.7</b>	<b>2179.7</b>	<b>2240.7</b>	<b>1744.0</b>	<b>1768.9</b>

Table 10. **Effectiveness of INTER on different parameter scales.**

method	InstructBLIP [13]	LLaVA-v1.5 (7B) [38]	Qwen-VL [3]	mPLUG-owl2 [63]
	[13]	(7B) [38]	[3]	[63]
○ Nucleus [23]	77.0	79.1	76.1	76.8
● Nucleus+INTER	<b>81.9</b>	<b>84.3</b>	<b>81.9</b>	<b>80.2</b>
○ Greedy [49]	81.3	85.1	79.4	80.9
● Greedy+INTER	<b>82.2</b>	<b>85.2</b>	<b>81.4</b>	<b>80.9</b>
○ Beam [4, 21, 53]	81.4	84.7	79.7	80.2
● Beam+INTER	<b>83.3</b>	<b>84.7</b>	<b>81.2</b>	<b>81.0</b>
○ VCD* [16]	80.6	82.7	82.3	79.7
● VCD*+INTER	<b>80.9</b>	<b>83.6</b>	<b>82.0</b>	<b>79.5</b>
○ OPERA <sup>†</sup> [25]	81.3	84.9	79.8	80.4
● OPERA <sup>†</sup> +INTER	<b>82.5</b>	<b>85.8</b>	<b>83.1</b>	<b>81.1</b>

Table 11. **Evaluating the performance of INTER’s correction on four decoding strategies** by the mean F1-score across various partitions of GQA [26]. Higher values are better.

## 11. Effectiveness at Different Parameter Scales.

Our evaluation establishes INTER’s cross-scale adaptability through validation across scales spanning 1B to 26B parameters. As shown in Table 10, the MME [19] benchmark reveals consistent performance improvements across diverse scales, demonstrating scaling-agnostic generalization capabilities.

## 12. Result on POPE

In this subsection, we evaluate the performance of the proposed INTER on the GQA [26] dataset within the POPE benchmark. The results, as shown in the Tab. 11, indicate that significant performance improvements across four models. Furthermore, these enhancements are consistent with the results on the MSCOCO [35] and AOKVQA [47] datasets, further validating the effectiveness and robustness of our approach.

## 13. Result on MME

In addition to demonstrating the performance improvements brought by INTER across various decoding strategies in 14 subtasks, we also conducted comparisons in terms of the total score and perception total score of MME [19]. As shown in Tab. 12, after correction with INTER, there was a maximum increase of over 343.7 points in the total score compared to Nucleus Sampling, and a maximum increase

of over 311.2 points in the perception total score. Furthermore, it can be observed that there is a certain degree of improvement across different models and decoding strategies, indicating the effectiveness of INTER.

## 14. Result on MM-Bench

To illustrate the improvement of INTER on MM-Bench in more detail, we present the performance of each subtask in Tabs. 13, 19 and 20. As we can see, using INTER results in an improvement across various metrics. In addition, to validate the performance of INTER across different LVLMS, Tab. 14 presents the performance on mPLUG-owl2. It can be observed that there is a high consistency with LLaVA-v1.5, and INTER brings a certain degree of enhancement. Finally, detailed results of mPLUG-owl2 at each subtasks are also presented in Tabs. 21 and 22.

## 15. Result on MMStar

Likewise, to assess the effectiveness of INTER on MMStar, we also present the performance of each subtask on LLaVA-v1.5 (7B) [38] in Tabs. 15, 23 and 24. The results indicate that our approach achieves good performance across most subtasks. Although there is no improvement of the correction effects on VCD [16] and OPERA [25] in the ‘Math’, the correction results using INTER for ‘Nucleus’ outperform those of VCD, and the performance on Beam Search is better than OPERA.

In addition, we conducted comparative experiments on MMStar using mPLUG-owl2 in Tabs. 16, 25 and 26, and the results show that our method has a certain corrective effect across different LVLMS.

## 16. Result on Greedy Search

In Tabs. 11 to 26, we demonstrated the effectiveness of INTER in correcting the Greedy Search across various benchmarks. It is evident that there is a significant improvement across different benchmarks, indicating that our method INTER exhibits generalization capabilities in correcting various decoding strategies.

## 17. Result on LLaVA-Bench

To more intuitively demonstrate the performance of INTER, detailed case studies were conducted using LLaVA-Bench. In Figs. 11 to 13, examples of the captioning and complex reasoning task for each model are presented. The hallucination parts are highlighted in red.

In addition to case study, we also assessed the accuracy and detailedness of responses generated by various methods on the LLaVA-Bench dataset using GPT-4o [28]. As shown in the Fig. 10, the answers generated after applying INTER

method	InstructBLIP [13]		LLaVA-v1.5 (7B) [38]		Qwen-VL [3]		mPLUG-owl2 [63]	
	Perception Total	Total	Perception Total	Total	Perception Total	Total	Perception Total	Total
○ Nucleus [23]	984.4	1251.8	1279.2	1502.2	1216.6	1465.6	1266.3	1573.5
● Nucleus+INTER	1295.6 (↑311.2)	1595.5 (↑343.7)	1372.0 (↑92.8)	1731.6 (↑229.4)	1279.8 (↑63.2)	1542.9 (↑77.3)	1353.8 (↑87.5)	1641.7 (↑68.2)
○ Greedy [49]	1160.9	1419.8	1452.2	1750.4	1238.9	1512.5	1352.5	1709.3
● Greedy+INTER	1291.2 (↑130.3)	1593.3 (↑173.5)	1470.5 (↑18.3)	1761.3 (↑10.9)	1292.4 (↑53.5)	1544.2 (↑31.7)	1360.4 (↑7.9)	1731.4 (↑22.1)
○ Beam [4, 21, 53]	1128.9	1318.6	1409.4	1707.2	1229.5	1513.4	1358.4	1710.5
● Beam+INTER	1281.8 (↑152.9)	1562.2 (↑243.6)	1438.3 (↑28.9)	1744.0 (↑36.8)	1271.5 (↑42.0)	1575.0 (↑61.6)	1363.3 (↑4.9)	1716.1 (↑5.6)
○ VCD* [16]	1167.9	1487.1	1364.0	1716.0	1240.0	1546.5	1269.7	1573.0
● VCD*+INTER	1306.8 (↑138.9)	1605.0 (↑117.9)	1380.0 (↑16.0)	1749.6 (↑33.6)	1297.0 (↑57.0)	1575.6 (↑29.1)	1305.2 (↑35.5)	1626.2 (↑53.2)
○ OPERA <sup>†</sup> [25]	1137.5	1326.5	1430.8	1721.2	1228.8	1501.7	1357.6	1740.8
● OPERA <sup>†</sup> +INTER	1274.1 (↑136.6)	1567.0 (↑240.5)	1439.8 (↑9.0)	1727.4 (↑6.2)	1304.0 (↑75.2)	1564.4 (↑62.7)	1377.7 (↑20.1)	1741.7 (↑0.9)

Table 12. **The total scores and perceptual total scores on MME [19].** ↑ means that higher values indicate lower hallucination levels. Results showed that the addition of INTER led to a certain degree of mitigating hallucinations for all decoding strategies.

#### GPT-4o Prompt

You are an AI tasked with evaluating and scoring the performance of two AI assistants in describing a specified image. Your evaluation will primarily focus on accuracy and detail in their descriptions. Accuracy will be assessed by identifying any hallucinations—elements of the description that do not align with the image and the related question. For detail, consider how comprehensive and rich the response is, excluding any hallucinated content. You will score each assistant on a scale from 1 to 10 based on these criteria. After scoring, you will provide an unbiased explanation of your evaluations, ensuring that your analysis is not influenced by the order in which the responses are presented.

#### Input format:

[Assistant 1]  
{Response 1}  
[End of Assistant 1]  
[Assistant 2]  
{Response 2}  
[End of Assistant 2]

#### Output format:

Accuracy: <Scores of the two responses>  
Reason:  
Detailedness: <Scores of the two responses>  
Reason:

Figure 9. Prompts of GPT-4o [28] for evaluations.

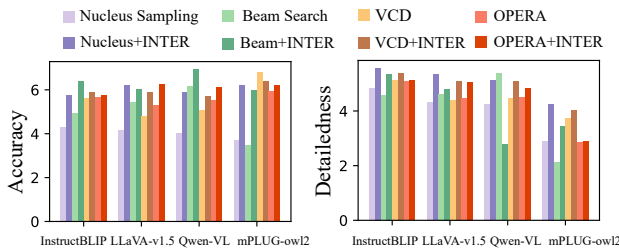


Figure 10. **Evaluating accuracy and detailedness on response of 60 Image-Text pairs in LLaVA-Bench [37] using GPT-4o [28].**

calibration received higher scores. The template of prompt is shown in Fig. 9.

## 18. Computation Efficiency

Similar to VCD [16], which require additional forward passes, INTER also necessitates extra inference to compute the logits under different subsets of  $A$ . While INTER increases the total number of forward passes, the actual runtime overhead remains negligible due to the capability of compressing all subset evaluations into a single batch.



**Prompt:** Explain all the cues that indicate the current traffic conditions.

**Category:** complex

**Nucleus:** The image captures a busy city highway with heavy traffic, featuring numerous cars and trucks. The traffic lights control the flow of vehicles, which can be seen in various positions along the highway, both near and far. There are at **least 20 traffic lights visible in the image**, illustrating the high volume of vehicles and the well-maintained traffic control system. The presence of traffic lights along the highway suggests that the area is likely heavily congested and that drivers need to follow the traffic lights to prevent accidents and maintain order on the road. Furthermore, the nighttime setting implies that the traffic is active during typical rush hours, adding to the overall impression of considerable traffic congestion in the area.

**VCD:** In the image, the current traffic conditions are indicated by the numerous cars and trucks moving down the freeway at night. The vehicles are packed tightly together, with some cars and trucks visible in the foreground and others further back, creating a dense traffic situation. The darkness of the night adds to the feeling of congestion, as it is more difficult for drivers to see each other and maintain safe distances between their vehicles. The **traffic lights** also help guide the flow of traffic, but the heavy volume of vehicles and limited visibility make this nighttime commute a challenging one for drivers.

**OPERA:** In the image, the traffic conditions are quite congested, as evidenced by the numerous cars and trucks on the road. The vehicles are lined up in both directions, with some cars and trucks occupying the left side of the road, while others are on the right side. The congestion is further emphasized by the presence of multiple traffic lights, indicating that this is an urban area with a well-regulated traffic system. **The traffic lights** are scattered throughout the scene, with some located closer to the foreground and others further in the background. The combination of the large number of vehicles and the presence of traffic lights suggests that this is a busy and congested city street at night.

**INTER:** In the image, the cues that indicate the current traffic conditions include a large number of cars and trucks traveling on a busy highway at night. The vehicles are moving in both directions, creating a sense of congestion and slow-moving traffic. The presence of multiple cars and trucks, as well as the nighttime setting, suggest that this is a typical rush hour or peak travel time when people are commuting to and from work, school, or other destinations. The heavy traffic can lead to longer travel times, increased fuel consumption, and higher stress levels for drivers and passengers alike.



**Prompt:** Describe this photo in detail.

**Category:** detail

**Nucleus:** The image displays an open refrigerator with a variety of food items stored inside, including several milk bottles. There are **five bottles in total**, arranged throughout the fridge in different sections, suggesting a well-stocked and organized kitchen space. Additionally, there is an open box on a shelf displaying many different fruits. There are carrots inside the box, **as well as a group of oranges**. A bowl is located close to the left side, perhaps holding more fruits. There are two cups visible in the bottom right corner, placed separately, and possibly **used for consuming the food items**.

**VCD:** The image displays an open refrigerator filled with various food items. The refrigerator is packed with fresh fruits and vegetables, including **carrots, strawberries, apples, and bananas**. The carrots are arranged on the left side, with strawberries occupying the right side of the refrigerator. In addition to the fruits and vegetables, the refrigerator also contains dairy products such as a milk carton and **a juice box**. These items are scattered throughout the refrigerator, with the juice box placed on the left side and the milk carton closer to the center. The open door allows us to view the well-stocked and organized interior of the refrigerator.

**OPERA:** The image displays an open refrigerator filled with a variety of food items. The refrigerator is packed with numerous bottles, some of which are placed on **the top shelves** and others on the bottom shelves. In addition to the bottles, there are several carrots scattered throughout the refrigerator, with some located on the top shelves and others on the bottom shelves. A bowl can also be seen in the refrigerator, placed on one of the top shelves. The refrigerator appears to be well-stocked and organized, making it easy to find and access the food stored in the appliance.

**INTER:** The image features a refrigerator filled with a variety of food items. The refrigerator is packed with multiple containers, bottles, and other food items, creating a full view of the contents inside. There are several bottles placed in different areas of the refrigerator, with one on the left side, one near the top right corner, and another one positioned towards the middle-right section of the fridge. A bowl is placed in the lower part of the refrigerator, towards the left side. Additionally, the refrigerator contains a pile of carrots. The carrots are situated on the left side of the refrigerator, occupying the lower portion.

Figure 11. Case study on LLaVA-v1.5 through LLaVA-Bench. Hallucinations are marked in red.





**Prompt:** In what other ways might someone express the same sentiment that this meme is expressing?

**Category:** complex

**Nucleus:** The scene of the man and woman standing on a boat while hailing at the camera symbolizes a vulnerable moment in the context of the movie. In the unreleased Pirates of the Caribbean sequel, this particular image captures the genuine emotion and vulnerability as the characters **Jack and Lois** are separated from the rest of their companions, stranded in the midst of a turbulent ocean. This creates tension and anticipation as the audience waits to see how the characters will handle this perilous situation, emphasizing the challenges they will face while attempting to find their way back to their destination.

**VCD:** The scene of a man and a woman standing on a boat and **holding onto each other with their arms around each other** is significant in the context of the movie because it is a romantic moment. It signifies the bond and connection between the two characters and the development of their relationship. This moment can be seen as a turning point in their story, where their love and trust in each other become stronger, leading to a deeper connection. In movies, such scenes are often used to create an emotional connection with the audience and to emphasize the importance of love and companionship in the characters' lives.

**OPERA:** In the context of the movie "Titanic," this scene is significant because it captures the romantic moment between the two main characters, Jack and Rose, as they share their first kiss on the back of the boat. This scene is iconic and memorable, as it symbolizes the beginning of their love story and sets the tone for the rest of the movie. The image of Jack and Rose embracing each other on the boat, with the sunset in the background, evokes a sense of romance, adventure, and the enduring power of love.

**INTER:** In the context of the movie "Titanic," this scene is significant because it captures the romantic moment between the two main characters, Jack and Rose, as they share their first kiss on the ship's deck. This scene is iconic and memorable, as it represents the beginning of their love story and sets the tone for the rest of the movie. It also highlights the beauty of the ship and the breathtaking view of the ocean, which adds to the overall atmosphere and emotional impact of the scene.



**Prompt:** Please explain the meme in detail.

**Category:** detail

**Nucleus:** The image portrays a pug dog laying comfortably on the floor on a blue wood floor. The dog appears to be asleep or just resting. The scene is edited to include a funny-looking remark, stating that the dog is "just Monday." This phrase is displayed in the bottom part of the image and appears in a speech bubble, **giving an amusing touch to the scene. The size and placement of the dog are proportionately respected with the writing.**

**VCD:** The image shows a small, cute dog laying on its side on a wooden floor, seemingly exhausted or napping. The dog appears to be a puppy, and it is positioned on a wooden floor that is part of a deck. The scene is set against a light blue background. Below the dog, the words "Just Monday..." are displayed, adding a **playful and humorous touch to the scene.** The combination of the dog's adorable appearance and the light-hearted commentary creates a **fun and entertaining meme.**

**OPERA:** The image features a small brown dog lying down on a wooden floor, possibly a porch or a deck. The dog appears to be sleeping or resting comfortably. The scene is accompanied by a caption that reads "Monday. Just Monday." This meme is likely meant to convey a **sense of relaxation or a break** from the hustle and bustle of everyday life, as the dog seems to be enjoying its time on the floor.

**INTER:** The image features a small brown dog lying down on a wooden floor. The dog appears to be sleeping or resting, taking up a significant portion of the floor. Above the dog, there is a caption that reads, "Monday. Just... Monday." This meme is likely meant to convey the feeling of being tired or unenthusiastic about the start of a new week.

Figure 12. Case study on mPLUG-owl2 through LLaVA-Bench. Hallucinations are marked in red.



**Prompt:** Show me a detailed recipe for cooking this at home.

**Category:** complex

**Nucleus:** The image features a delicious sandwich cut into two equal halves to serve as subs. A green Subway logo is placed over the top of one half, emphasizing its originality and promoting their signature substyle dishes available there in this particular menu item called "Steak & Cheese!". In addition to these famous deli meats like ham or maybe salami inside each slice's bread roll with lettuce on both sides before adding slices from steaming grilled chicken breast!

**VCD:** The image features two cut subway sandwiches placed side by side on a dark background. Each sub is loaded with meats, lettuce, and possibly other vegetables, making it an appetizing dish to prepare at home. Subway's footlong sandwiches are popular choices for customers who crave a filling and tasty lunch option. These two subway sandwiches can be replicated easily using the ingredients you have available in your kitchen, ensuring that you can enjoy this satisfying meal anytime you want.

**OPERA:** The image features two sub sandwiches cut in half, placed on a black background. The sub sandwiches are loaded with various ingredients, including meat, lettuce, tomato, and cheese. The sandwiches are positioned close to each other, creating a visually appealing display. The sandwiches are likely from Subway, a popular fast-food chain known for its variety of sandwiches and fresh ingredients.

**INTER:** The sandwich is presented on a dark background, adding to the dramatic effect of the dish. The image captures the attention of anyone who appreciates high-quality, mouth-watering sandwiches. In order to recreate this dish at home, follow the steps below: 1. Start with a freshly baked or toasted sub roll. 2. Spread mayonnaise on the inside of the roll. 3. Layer on the desired fillings, such as meats, cheese, and lettuce. 4. Close the sandwich by placing the halves together, sealing the fillings in. 5. Enjoy your homemade, mouth-watering Subway-style sandwich!



**Prompt:** Please explain the meme in detail.

**Category:** detail

**Nucleus:** The image features a painting of an artistic portrayal, where dogs have been incorporated into the portrait. A dog can be seen standing in front and center on his two hind legs behind Da Vinci's Mona Lisa background scene-appearing as if he is her pet or co-star! In this clever composition by artist Chloe Jeavons Gardner based off one known most famous paintings from history "Mona", she added small details to pay homage both historic beauty while using contemporary touches like adding doggies at bottom right corner which makes it even more charismatic piece for sure!

**VCD:** The image features a dog dressed as Leonardo da Vinci's Mona Lisa. The dog is wearing a long, brown dress and appears to be looking directly at the viewer with its eyes. It's placed in front of an oil painting backdrop that resembles the famous artwork. In total, there are five dogs visible in the scene. Three of them can be found near the edges, while one sits on top of the other two towards the middle of the image.

**OPERA:** The image features a painting of a dog dressed up as Mona Lisa, the famous painting by Leonardo da Vinci. The dog is depicted in the style of the original Mona Lisa painting, with its head positioned towards the right side of the image and its body slightly tilted to the left. The painting captures the essence of the original Mona Lisa, while adding a unique twist by featuring a dog as the subject.

**INTER:** The image features a large, long-haired dog dressed up as Leonardo da Vinci's famous painting, "Mona Lisa". The dog, likely a dachshund, has been transformed into an artwork, complete with its own crown. It's clear that the artist put a lot of effort into creating this unique and intriguing piece.

Figure 13. Case study on InstructBLIP through LLaVA-Bench. Hallucinations are marked in red.

method	Overall	AR	CP	FP-C	FP-S	LR	RR
◦ Nucleus [23]	57.3	50.0	73.0	48.8	58.1	44.7	52.6
● Nucleus+INTER	<b>62.6</b>	<b>57.0</b>	<b>76.4</b>	<b>52.0</b>	<b>65.0</b>	<b>48.3</b>	<b>63.2</b>
◦ Greedy [49]	65.2	58.4	77.8	55.3	69.3	50.7	64.7
● Greedy+INTER	<b>65.2</b>	<b>58.4</b>	<b>77.8</b>	<b>55.3</b>	<b>69.3</b>	<b>50.7</b>	<b>64.7</b>
◦ Beam [4, 21, 53]	65.1	57.8	77.8	55.3	69.3	50.7	64.7
● Beam+INTER	<b>65.1</b>	<b>58.1</b>	<b>77.8</b>	<b>55.3</b>	<b>69.3</b>	<b>50.7</b>	<b>64.7</b>
◦ VCD* [16]	62.5	54.7	77.5	53.4	64.9	48.5	60.5
● VCD*+INTER	<b>62.9</b>	<b>54.7</b>	<b>77.6</b>	52.3	<b>66.0</b>	47.6	<b>65.0</b>
◦ OPERA <sup>†</sup> [25]	65.0	57.8	77.8	55.3	69.0	50.7	64.7
● OPERA <sup>†</sup> +INTER	<b>65.0</b>	<b>57.8</b>	<b>77.9</b>	55.1	<b>69.0</b>	<b>50.7</b>	<b>64.7</b>

Table 13. Validation of INTER on MM-Bench [39] using LLaVA-v1.5 (7B) [38].

method	Overall	AR	CP	FP-C	FP-S	LR	RR
◦ Nucleus [23]	57.0	51.1	72.2	41.5	59.9	44.6	55.3
● Nucleus+INTER	<b>61.4</b>	<b>57.6</b>	<b>74.4</b>	<b>41.7</b>	<b>62.8</b>	<b>46.9</b>	<b>60.8</b>
◦ Greedy [49]	63.5	55.4	77.5	52.2	65.8	49.1	70.7
● Greedy+INTER	62.3	<b>56.3</b>	75.7	49.3	65.3	<b>49.3</b>	64.7
◦ Beam [4, 21, 53]	63.5	55.4	77.5	52.2	65.8	49.8	69.2
● Beam+INTER	<b>63.7</b>	<b>55.6</b>	<b>77.5</b>	<b>52.4</b>	<b>65.9</b>	<b>49.8</b>	<b>70.7</b>
◦ VCD* [16]	59.2	52.1	75.1	43.7	62.1	45.9	59.0
● VCD*+INTER	<b>59.5</b>	<b>53.6</b>	74.1	<b>44.3</b>	<b>62.4</b>	<b>48.0</b>	58.3
◦ OPERA <sup>†</sup> [25]	63.4	55.4	77.5	52.2	65.8	49.1	69.2
● OPERA <sup>†</sup> +INTER	<b>63.6</b>	<b>55.4</b>	<b>77.5</b>	<b>52.3</b>	65.7	<b>49.8</b>	<b>70.9</b>

Table 14. Validation of INTER on MM-Bench [39] using mPLUG-owl2 [63].

method	Avg.	CP	FP	IR	LR	ST	MA
◦ Nucleus [23]	29.3	52.8	22.4	38.0	22.8	17.6	22.4
● Nucleus+INTER	<b>31.9</b>	<b>58.0</b>	<b>29.8</b>	<b>39.4</b>	<b>27.6</b>	15.4	<b>22.8</b>
◦ Greedy [49]	30.7	59.2	24.8	40.0	27.2	13.6	19.6
● Greedy+INTER	<b>31.9</b>	55.2	<b>29.2</b>	<b>45.2</b>	<b>29.2</b>	<b>15.2</b>	17.6
◦ Beam [4, 21, 53]	31.1	58.4	22.8	40.4	28.8	14.8	21.2
● Beam+INTER	<b>31.7</b>	54.8	<b>30.4</b>	<b>44.0</b>	26.0	<b>18.4</b>	16.4
◦ VCD* [16]	30.3	54.4	24.4	38.0	26.0	16.8	22.4
● VCD*+INTER	<b>31.1</b>	<b>55.6</b>	<b>26.8</b>	<b>40.0</b>	<b>28.8</b>	15.2	20.4
◦ OPERA <sup>†</sup> [25]	31.4	59.2	23.6	40.8	28.8	14.8	21.2
● OPERA <sup>†</sup> +INTER	<b>32.9</b>	56.8	<b>30.0</b>	<b>42.4</b>	<b>28.8</b>	<b>18.8</b>	20.8

Table 15. Validation of INTER on MMStar [7] using LLaVA-v1.5 (7B) [38].

method	Avg.	CP	FP	IR	LR	ST	MA
◦ Nucleus [23]	30.5	50.4	24.8	40.0	27.6	17.6	22.4
● Nucleus+INTER	<b>32.3</b>	<b>53.2</b>	<b>25.2</b>	<b>42.0</b>	<b>31.6</b>	<b>18.0</b>	<b>23.6</b>
◦ Greedy [49]	30.1	53.2	26.0	40.4	28.8	12.0	20.0
● Greedy+INTER	<b>33.3</b>	<b>55.2</b>	<b>29.6</b>	<b>42.4</b>	<b>30.8</b>	<b>17.2</b>	<b>24.8</b>
◦ Beam [4, 21, 53]	30.7	52.4	26.0	42.0	28.8	12.0	23.2
● Beam+INTER	30.5	<b>52.8</b>	24.4	39.2	<b>29.6</b>	<b>14.0</b>	22.8
◦ VCD* [16]	31.5	52.8	26.8	36.0	25.6	18.8	28.8
● VCD*+INTER	<b>32.3</b>	<b>52.8</b>	25.6	<b>39.6</b>	<b>32.0</b>	17.2	26.8
◦ OPERA <sup>†</sup> [25]	30.5	52.8	26.4	41.6	28.4	12.0	22.0
● OPERA <sup>†</sup> +INTER	<b>30.9</b>	<b>52.8</b>	24.4	39.6	<b>29.6</b>	<b>14.8</b>	<b>24.0</b>

Table 16. Validation of INTER on MMStar [7] using mPLUG-owl2 [63].

method	InstructBLIP [13]		LLaVA-v1.5 (7B) [38]		Qwen-VL [3]		mPLUG-owl2 [63]	
	COCO [35]	AOKVQA [47]	COCO [35]	AOKVQA [47]	COCO [35]	AOKVQA [47]	COCO [35]	AOKVQA [47]
○ Greedy [49]	84.4	81.3	84.5	84.3	83.4	85.0	83.4	81.3
● Greedy+INTER	<b>85.1</b>	<b>83.7</b>	<b>86.4</b>	<b>84.4</b>	<b>86.0</b>	<b>86.4</b>	<b>83.4</b>	<b>81.7</b>

Table 17. **Evaluating the performance of INTER’s correction on Greedy Search [49]** by the mean F1-score across various partitions of two datasets in POPE [34]. Higher values are better.

Max Token	method	InstructBLIP [13]		LLaVA-v1.5 (7B) [38]		mPLUG-owl2 [63]	
		$C_S$	$C_I$	$C_S$	$C_I$	$C_S$	$C_I$
64	○ Greedy [49]	26.2	13.8	22.0	6.7	23.0	8.3
	● Greedy+INTER	<b>25.8</b>	<b>9.2</b>	<b>22.0</b>	<b>6.7</b>	<b>20.6</b>	<b>7.9</b>
512	○ Greedy [49]	49.2	21.9	48.8	13.4	58.2	18.5
	● Greedy+INTER	55.8	<b>18.1</b>	<b>48.8</b>	<b>13.4</b>	<b>54.4</b>	<b>17.9</b>

Table 18. **Evaluating the effectiveness of INTER in correcting Greedy Search** using LLaVA-v1.5 on CHAIR [46], with a maximum token length of 64 and 512. A smaller value indicates a lower degree of hallucinations.



method	Coarse Perception (CP)					Cross-instance Fine-grained Perception (FP-C)			Single-instance Fine-grained Perception (FP-S)			
	Image Emotion	Image Topic	Image Scene	Image Style	Image Quality	Action Recognition	Attribute Comparision	Spatial Realtionship	Celebrity Recognition	Object Localization	Attribute Recognition	OCR
○ Nucleus [23]	71.0	76.4	94.1	66.5	24.7	82.3	44.0	11.9	75.5	25.7	73.5	53.2
● Nucleus+INTER	<b>77.5</b>	<b>80.7</b>	<b>96.1</b>	<b>70.8</b>	<b>25.3</b>	<b>84.7</b>	<b>51.1</b>	<b>13.0</b>	<b>80.1</b>	<b>35.2</b>	<b>81.4</b>	<b>59.0</b>
○ Greedy [49]	78.0	81.4	96.1	75.5	28.0	87.0	53.2	18.6	81.8	44.8	86.0	59.0
● Greedy+INTER	<b>78.0</b>	<b>81.4</b>	<b>96.1</b>	<b>75.5</b>	<b>28.0</b>	<b>87.0</b>	<b>53.2</b>	<b>18.6</b>	<b>81.8</b>	<b>44.8</b>	<b>86.0</b>	<b>59.0</b>
○ Beam [4, 21, 53]	78.0	81.4	96.1	75.5	28.0	87.0	53.2	18.6	81.8	44.8	86.0	59.0
● Beam+INTER	<b>78.0</b>	<b>81.4</b>	<b>96.1</b>	<b>75.5</b>	<b>28.0</b>	<b>87.0</b>	<b>53.2</b>	<b>18.6</b>	<b>81.8</b>	<b>44.8</b>	<b>86.0</b>	<b>59.0</b>
○ VCD* [16]	77.0	81.4	96.1	77.0	25.3	86.1	49.0	17.5	78.3	37.1	81.8	58.3
● VCD*+INTER	<b>77.0</b>	<b>82.1</b>	<b>96.1</b>	<b>75.0</b>	<b>28.0</b>	<b>84.7</b>	<b>48.9</b>	<b>15.8</b>	<b>80.3</b>	<b>37.8</b>	<b>81.1</b>	<b>60.9</b>
○ OPERA <sup>†</sup> [25]	78.0	81.4	96.1	75.5	28.0	87.0	53.2	18.6	81.8	43.5	86.0	59.0
● OPERA <sup>†</sup> +INTER	<b>78.0</b>	<b>81.4</b>	<b>96.1</b>	<b>75.9</b>	<b>28.0</b>	<b>87.0</b>	<b>53.2</b>	<b>17.9</b>	<b>81.8</b>	<b>43.5</b>	<b>86.0</b>	<b>59.0</b>

Table 19. Evaluating the performance of INTER on MM-Bench [39] using LLaVA-v1.5 (7B) [38], focusing on coarse perception and fine-grained perception subtasks.

method	Attribute Reasoning (AR)				Logic Reasoning (LR)		Relation Reasoning (RR)		
	Physical Property	Function Reasoning	Nature Relation	Future Prediction	Structuralized Image -Text Understanding	Identity Reasoning	Social Relation	Physical Relation	
○ Nucleus [23]	39.3	68.8	31.3	31.5	20.6	93.2	72.1	17.0	
● Nucleus+INTER	<b>44.3</b>	<b>77.3</b>	<b>38.0</b>	<b>39.2</b>	<b>24.1</b>	<b>93.8</b>	<b>85.5</b>	<b>22.3</b>	
○ Greedy [49]	43.8	82.9	34.6	41.5	27.0	95.5	86.1	25.5	
● Greedy+INTER	<b>43.8</b>	<b>82.9</b>	<b>34.6</b>	<b>41.5</b>	<b>27.0</b>	<b>95.5</b>	<b>86.1</b>	<b>25.5</b>	
○ Beam [4, 21, 53]	43.8	81.6	34.6	41.5	27.0	95.5	86.1	25.5	
● Beam+INTER	<b>43.8</b>	<b>82.2</b>	<b>34.6</b>	<b>41.5</b>	<b>27.0</b>	<b>95.5</b>	<b>86.1</b>	<b>25.5</b>	
○ VCD* [16]	41.1	73.7	39.1	40.0	23.1	95.5	83.7	18.1	
● VCD*+INTER	<b>41.1</b>	<b>73.7</b>	<b>39.1</b>	<b>39.2</b>	<b>23.4</b>	<b>92.6</b>	<b>88.4</b>	<b>22.3</b>	
○ OPERA <sup>†</sup> [25]	43.8	81.6	34.6	41.5	27.0	95.5	86.1	25.5	
● OPERA <sup>†</sup> +INTER	<b>43.8</b>	<b>81.6</b>	<b>34.6</b>	<b>41.5</b>	<b>27.0</b>	<b>95.5</b>	<b>86.1</b>	<b>25.5</b>	

Table 20. Evaluating the performance of INTER on MM-Bench [39] using LLaVA-v1.5 (7B) [38], focusing on attribute reasoning, logic reasoning and relation reasoning subtasks.

method	Coarse Perception (CP)					Cross-instance Fine-grained Perception (FP-C)			Single-instance Fine-grained Perception (FP-S)			
	Image Emotion	Image Topic	Image Scene	Image Style	Image Quality	Action Recognition	Attribute Comparision	Spatial Realtionship	Celebrity Recognition	Object Localization	Attribute Recognition	OCR
○ Nucleus [23]	70.5	75.7	94.1	67.5	18.7	70.7	27.7	17.0	79.8	24.4	70.5	62.8
● Nucleus+INTER	<b>71.0</b>	<b>77.0</b>	<b>96.1</b>	<b>73.1</b>	<b>19.3</b>	<b>71.2</b>	<b>29.1</b>	<b>15.9</b>	<b>81.1</b>	<b>29.2</b>	<b>73.9</b>	<b>65.4</b>
○ Greedy [49]	<b>76.0</b>	<b>76.4</b>	<b>97.1</b>	<b>81.1</b>	<b>22.7</b>	<b>77.7</b>	<b>46.8</b>	<b>25.4</b>	<b>82.8</b>	<b>34.6</b>	<b>73.9</b>	<b>71.8</b>
● Greedy+INTER	<b>76.0</b>	73.6	96.1	<b>83.0</b>	12.0	<b>79.5</b>	41.8	18.6	81.8	28.6	<b>80.3</b>	<b>71.8</b>
○ Beam [4, 21, 53]	76.0	76.4	97.1	81.1	22.7	77.7	46.8	25.4	82.8	34.6	73.9	71.8
● Beam+INTER	<b>76.0</b>	<b>76.4</b>	<b>97.1</b>	<b>81.1</b>	<b>22.7</b>	<b>77.7</b>	<b>47.1</b>	<b>26.0</b>	<b>82.8</b>	<b>34.7</b>	<b>74.1</b>	<b>71.8</b>
○ VCD* [16]	71.5	79.3	96.3	75.9	17.3	72.6	32.6	17.5	79.8	26.7	75.0	66.7
● VCD*+INTER	<b>72.5</b>	<b>73.6</b>	<b>96.0</b>	<b>78.8</b>	<b>10.7</b>	<b>74.9</b>	<b>33.3</b>	<b>15.8</b>	<b>81.3</b>	<b>25.2</b>	<b>75.4</b>	<b>68.0</b>
○ OPERA <sup>†</sup> [25]	76.0	76.4	97.1	81.1	22.7	77.7	46.8	25.4	82.8	34.6	73.9	71.8
● OPERA <sup>†</sup> +INTER	<b>76.0</b>	<b>76.4</b>	97.0	<b>81.1</b>	<b>22.7</b>	<b>78.0</b>	<b>46.8</b>	<b>25.4</b>	82.7	<b>34.6</b>	<b>73.9</b>	<b>71.8</b>

Table 21. Evaluating the performance of INTER on MM-Bench [39] using mPLUG-owl2 [63], focusing on coarse perception and fine-grained perception subtasks.

method	Attribute Reasoning (AR)				Logic Reasoning (LR)		Relation Reasoning (RR)	
	Physical Property	Function Reasoning	Nature Relation	Future Prediction	Structuralized Image -Text Understanding	Identity Reasoning	Social Relation	Physical Relation
○ Nucleus [23]	32.4	75.3	33.0	36.2	18.8	92.1	73.3	22.3
● Nucleus+INTER	<b>33.3</b>	<b>76.6</b>	<b>36.3</b>	<b>40.0</b>	<b>20.9</b>	<b>93.8</b>	<b>79.1</b>	<b>26.9</b>
○ Greedy [49]	33.3	82.2	36.9	45.4	23.1	93.8	88.4	38.3
● Greedy+INTER	<b>36.1</b>	79.1	<b>41.3</b>	<b>46.9</b>	21.3	<b>96.0</b>	86.1	25.5
○ Beam [4, 21, 53]	33.3	82.2	36.9	45.4	24.5	93.8	88.4	34.0
● Beam+INTER	<b>33.9</b>	<b>82.2</b>	<b>36.9</b>	<b>45.4</b>	<b>24.5</b>	<b>93.8</b>	<b>88.4</b>	<b>38.2</b>
○ VCD* [16]	32.0	75.3	37.4	36.9	20.9	92.6	77.3	25.5
● VCD*+INTER	<b>34.3</b>	<b>76.0</b>	<b>39.3</b>	<b>43.9</b>	<b>20.2</b>	<b>95.5</b>	<b>79.1</b>	<b>20.2</b>
○ OPERA <sup>†</sup> [25]	<b>33.3</b>	<b>82.2</b>	<b>36.9</b>	<b>45.4</b>	<b>23.1</b>	<b>93.8</b>	<b>88.4</b>	<b>34.0</b>
● OPERA <sup>†</sup> +INTER	<b>33.8</b>	82.1	<b>36.9</b>	<b>45.4</b>	<b>24.5</b>	<b>93.8</b>	<b>88.9</b>	<b>38.3</b>

Table 22. **Evaluating the performance of INTER on MM-Bench [39] using mPLUG-owl2 [63],** focusing on attribute reasoning, logic reasoning and relation reasoning subtasks.

method	Coarse Perception (CP)			Fine-grained Perception (FP)			Instance Reasoning (IR)		
	Image Scene & Topic	Image Style & Quality	Image Emotion	Object Counting	Recognition	Localization	Single-Instance Reasoning	Cross-Instance Attribute Reasoning	Cross-Instance Relation Reasoning
○ Nucleus [23]	45.4	66.7	51.6	17.4	25.4	25.0	56.6	29.2	21.0
● Nucleus+INTER	<b>48.2</b>	<b>73.1</b>	<b>58.1</b>	<b>25.0</b>	<b>37.3</b>	<b>27.5</b>	51.5	<b>33.7</b>	<b>32.3</b>
○ Greedy [49]	48.9	74.4	67.7	20.7	29.7	20.0	52.5	31.5	32.3
● Greedy+INTER	48.2	66.7	58.1	<b>32.6</b>	27.1	<b>27.5</b>	<b>56.6</b>	<b>34.8</b>	<b>41.9</b>
○ Beam [4, 21, 53]	48.9	71.8	67.7	21.7	25.4	17.5	51.5	28.1	40.3
● Beam+INTER	47.5	69.2	<b>67.7</b>	<b>26.1</b>	<b>27.1</b>	<b>27.5</b>	<b>56.6</b>	<b>28.1</b>	<b>41.9</b>
○ VCD* [16]	44.0	70.5	61.3	27.2	22.9	22.5	48.5	32.6	29.0
● VCD*+INTER	<b>47.5</b>	<b>70.5</b>	54.8	26.1	<b>28.8</b>	<b>22.5</b>	<b>52.5</b>	31.5	<b>32.3</b>
○ OPERA <sup>†</sup> [25]	49.6	73.1	67.7	22.8	26.3	17.5	52.5	31.5	35.5
● OPERA <sup>†</sup> +INTER	45.4	71.8	<b>67.7</b>	<b>31.5</b>	<b>31.4</b>	<b>20.0</b>	<b>56.6</b>	<b>31.5</b>	<b>37.1</b>

Table 23. **Evaluating the performance of INTER on MMStar [7] using LLaVA-v1.5 (7B) [38],** focusing on coarse perception, fine-grained perception and instance reasoning subtasks.

method	Logit Reasoning (LR)			Science and Technology (ST)			Math (MA)		
	Code Sequence Reasoning	Diagram Reasoning	Common Reasoning	Biology & Chemistry & Physics	Electronics & Energy & Mechanical eng.	Geography & Earth Science & Agriculture	Geometry	Numeric & Calculation	Commonsense & Statistical Reasoning
○ Nucleus [23]	23.1	19.1	26.7	16.7	20.5	20.7	19.8	33.3	27.7
● Nucleus+INTER	<b>25.6</b>	<b>19.1</b>	<b>34.7</b>	<b>16.0</b>	17.9	<b>20.7</b>	<b>30.2</b>	31.3	19.3
○ Greedy [49]	23.1	22.7	33.7	12.5	15.4	17.2	25.6	27.1	16.9
● Greedy+INTER	<b>23.1</b>	21.8	<b>39.6</b>	<b>15.3</b>	10.3	<b>20.7</b>	17.4	18.8	<b>24.1</b>
○ Beam [4, 21, 53]	33.3	24.5	31.7	13.2	12.8	22.4	25.6	31.3	19.3
● Beam+INTER	<b>35.9</b>	21.8	<b>32.7</b>	<b>16.0</b>	<b>25.6</b>	<b>27.6</b>	24.4	27.1	<b>22.9</b>
○ VCD* [16]	20.5	20.0	34.7	18.1	15.4	17.2	27.9	20.8	26.5
● VCD*+INTER	<b>23.1</b>	<b>23.6</b>	<b>36.6</b>	17.4	7.7	<b>17.2</b>	17.4	<b>27.1</b>	<b>27.7</b>
○ OPERA <sup>†</sup> [25]	33.3	24.5	31.7	13.2	12.8	22.4	25.6	31.3	19.3
● OPERA <sup>†</sup> +INTER	<b>35.9</b>	21.8	<b>31.7</b>	<b>15.3</b>	<b>25.6</b>	<b>27.6</b>	23.3	27.1	<b>22.9</b>

Table 24. **Evaluating the performance of INTER on MMStar [7] using LLaVA-v1.5 (7B) [38],** focusing on logit reasoning, science technology and math capability subtasks.

method	Coarse Perception (CP)			Fine-grained Perception (FP)			Instance Reasoning (IR)		
	Image Scene & Topic	Image Style & Quality	Image Emotion	Object Counting	Recognition	Localization	Single-Instance Reasoning	Cross-Instance Attribute Reasoning	Cross-Instance Relation Reasoning
○ Nucleus [23]	43.9	56.4	64.5	27.2	24.6	20.0	49.5	28.1	41.9
● Nucleus+INTER	<b>47.5</b>	<b>58.9</b>	<b>70.9</b>	<b>31.5</b>	<b>27.9</b>	15.0	<b>53.5</b>	<b>31.5</b>	30.6
○ Greedy [49]	46.1	59.0	71.0	26.1	30.5	12.5	53.5	30.3	33.9
● Greedy+INTER	<b>48.9</b>	<b>61.5</b>	67.7	<b>33.7</b>	29.7	<b>20.0</b>	<b>55.6</b>	<b>32.6</b>	<b>35.5</b>
○ Beam [4, 21, 53]	45.4	57.7	70.9	27.2	29.7	12.5	53.5	29.2	41.9
● Beam+INTER	<b>46.1</b>	<b>57.7</b>	<b>70.9</b>	<b>28.2</b>	26.3	10.0	<b>53.5</b>	28.1	32.3
○ VCD* [16]	46.8	58.9	64.5	27.2	28.2	20.0	46.5	28.1	30.6
● VCD*+INTER	<b>47.5</b>	56.4	<b>67.7</b>	<b>28.3</b>	24.6	<b>22.5</b>	<b>51.5</b>	<b>30.3</b>	<b>33.9</b>
○ OPERA <sup>†</sup> [25]	45.4	58.9	70.9	27.2	29.7	15.0	53.5	29.2	40.3
● OPERA <sup>†</sup> +INTER	<b>46.1</b>	57.7	70.9	<b>28.3</b>	26.3	10.0	<b>53.5</b>	28.1	33.9

Table 25. Evaluating the performance of INTER on MMStar [7] using mPLUG-owl2 [63], focusing on coarse perception, fine-grained perception and instance reasoning subtasks.

method	Logit Reasoning (LR)			Science and Technology (ST)			Math (MA)		
	Code Sequence Reasoning	Diagram Reasoning	Common Reasoning	Biology & Chemistry & Physics	Electronics & Energy & Mechanical eng.	Geography & Earth Science & Agriculture	Geometry	Numeric Commonsense & Calculation	Statistical Reasoning
○ Nucleus [23]	25.6	21.8	34.7	15.1	21.7	20.7	22.4	22.9	22.1
● Nucleus+INTER	12.8	18.2	<b>42.6</b>	<b>19.2</b>	<b>36.9</b>	<b>24.1</b>	<b>19.8</b>	<b>20.8</b>	<b>26.7</b>
○ Greedy [49]	30.8	24.6	32.7	11.0	8.7	17.2	18.1	25.0	19.8
● Greedy+INTER	20.5	<b>24.6</b>	<b>41.6</b>	<b>15.8</b>	<b>23.9</b>	15.5	<b>19.0</b>	<b>27.1</b>	<b>31.4</b>
○ Beam [4, 21, 53]	25.6	25.5	33.7	11.6	6.5	17.2	18.9	25.0	27.9
● Beam+INTER	<b>25.6</b>	24.5	<b>36.6</b>	<b>12.3</b>	<b>15.2</b>	<b>17.2</b>	<b>19.8</b>	22.9	26.7
○ VCD* [16]	28.2	20.9	29.7	23.3	10.9	13.8	23.3	33.7	33.7
● VCD*+INTER	17.9	<b>25.5</b>	<b>44.6</b>	15.8	<b>21.7</b>	<b>17.2</b>	<b>25.0</b>	27.1	29.1
○ OPERA <sup>†</sup> [25]	25.6	23.6	34.7	11.6	6.5	17.2	19.0	25.0	24.4
● OPERA <sup>†</sup> +INTER	<b>25.6</b>	<b>25.5</b>	<b>35.6</b>	<b>13.0</b>	<b>17.4</b>	<b>17.2</b>	<b>21.6</b>	<b>25.0</b>	<b>26.7</b>

Table 26. Evaluating the performance of INTER on MMStar [7] using mPLUG-owl2 [63], focusing on logit reasoning, science, technology, and math capability subtasks.